4-9-2018

Understanding long-term variations in surface ozone in United States (U.S.) National Parks

Deborah McGlynn
dfmcglyn@syr.edu

UNDERSTANDING LONG-TERM VARIATIONS IN SURFACE OZONE IN UNITED STATES (U.S.) NATIONAL PARKS

by

Deborah F. McGlynn

A thesis
submitted in partial fulfillment
of the requirements for the
Master of Science Degree
State University of New York
College of Environmental Science and Forestry
Syracuse, New York
April 2018

Department of Chemistry

Approved by:
Huiting Mao, Major Professor
Douglas Johnston, Chair, Examining Committee
Ivan I. Gitsov, Department Chair
S. Scott Shannon, Dean, The Graduate School

Acknowledgements

I would like to thank my advisor, Dr. Huiting Mao for her guidance and support over the past three years. This work would not have been possible without her mentorship through every step of this process. I would also like to thank Dr. Barkley Sive and Dr. Zaohua Wu for their thoughts and input on matters pertaining to some findings in this work.

Bradley Sutliff and Dominique Derminio listened to a number of presentations of this work and were instrumental in fine-tuning my thoughts and presentations. They, as well as the members of my lab, were very supportive throughout this process and served as a sounding board when difficulties arose.

Lastly, I would like to thank my parents, sister, and Bradley Sutliff. I would not be where I am today without them.

This thesis was in part supported by the National Park Service.

Table of Contents

List of Figures

List of Tables

Abbreviations

AO – Arctic Oscillation

CH_4 – methane

CO – carbon monoxide

ECMWF – European Center for Medium Range Weather Forecasting

EEMD – Ensemble Empirical Mode Decomposition

ENSO – El Niño Southern Oscillation

EOF – Empirical Orthogonal Function

EPA – Environmental Protection Agency

HO_2 – peroxy radical

hPa – hectopascal

HYSPLIT – Hybrid Single Particle Lagrangian Integrated Trajectory Model

IMF – intrinsic mode function

IPCC – Intergovernmental Panel on Climate Change

NAAQS – National Ambient Air Quality Standards

NAO – North Atlantic Oscillation

NCAR – National Center for Atmospheric Research

NCEP – National Center for Environmental Protection

NMVOC – non-methane volatile organic compound

NOAA – National Oceanic and Atmospheric Administration

NO_x – oxides of nitrogen, including NO and NO_2

NPS – National Park Service

NPS GPMP – National Park Service Gaseous Pollutant Monitoring Program

O_3 – ozone

OH – hydroxy radical

OLR – Ordinary Linear Regression

PDO – Pacific Decadal Oscillation

ppbv – parts per billion by volume

ppmv – parts per million by volume

PRB – Policy Relevant Background

R_n – residual of trend with n number of data points

SST – sea surface temperature

VOC – volatile organic compound

Abstract

D. F. McGlynn. Understanding long-term variations in surface ozone in United States (U.S.) National Parks. 95 pages, 2 tables, 10 figures, 2018. Atmosphere style guide used.

In the troposphere, surface ozone is an air pollutant that has deleterious effects on human respiratory function and crop yields. Therefore, an understanding of spatial and temporal ozone concentration changes is necessary. The Ensemble Empirical Mode Decomposition (EEMD) method was used to analyze processes on varying time scales for surface ozone data from 25 U.S. National Park Service sites. Time scales of interest include the seasonal cycle, large-scale climate oscillations, and long-term (>10 years) trends. Variability in each of these oscillatory components is determined. Further analysis was done at one site after initial analyses yielded findings disparate from the rest of the study pool. For this site (DENA-HQ) variability in the El Niño Southern Oscillation and Pacific Decadal Oscillation was shown to affect the trajectory of pollutants to the site. The findings from this study can assist predictions regarding the timing and amplitude of peak ozone across the US and inform policy makers where emission reductions have been effective, enlightening future policy decisions.

Keywords: ozone; trends; Ensemble Empirical Mode Decomposition; seasonal cycle; El Niño Southern Oscillation; Pacific Decadal Oscillation; National Park Service

D.F. McGlynn
Candidate for the degree of Master of Science, April 2018
Huiting Mao, Ph.D.
Department of Chemistry
State University of New York College of Environmental Science and Forestry
Syracuse, New York

Chapter 1: Introduction

The atmosphere is comprised of many gaseous compounds. The lowest of the 5 layers of the atmosphere, the troposphere, contains 75% of the atmosphere's mass. Anthropogenic activities heavily influence this layer, making it the subject of many scientific and political discussions and regulations. Anthropogenic emissions have long affected atmospheric composition, visibility, and meteorological factors such as temperature [1]. In the troposphere, ozone (O_3), is of great concern due to its negative effects on human health, vegetation, and agricultural crops [1].

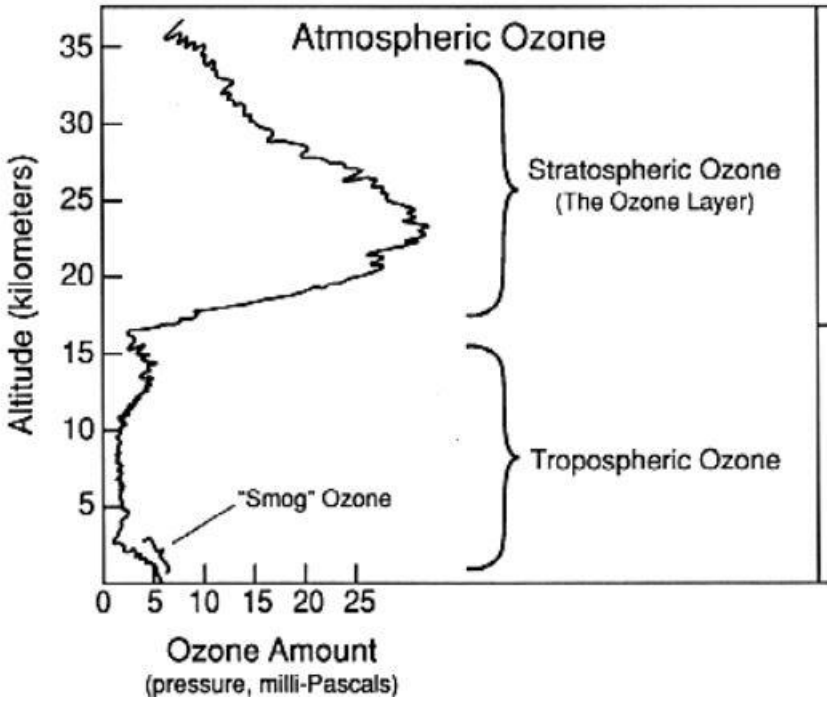

Figure 1.1: Concentration of ozone within the stratosphere and troposphere. A large stratospheric ozone layer occurs above the troposphere while the presence of "smog" can be seen in the lowest portion of the troposphere. This figure has been adapted from the National Oceanic and Atmospheric Administration [2].

An ozone layer naturally forms in the stratosphere, the layer above the troposphere **(**Figure 1.1**)**. This layer shields the biosphere from harmful UV radiation [2]. Concentrations of tropospheric ozone are lower than concentrations of ozone in the stratosphere. In the

troposphere, ozone is a secondary air pollutant because it readily forms when its precursor emissions of volatile organic compounds (VOCs) and nitrogen oxides (NO_x) are exposed to abundant sunlight [3,4]. This mixes with aerosols and particulate matter to form a "smog" layer at the surface of the earth (Figure 1.1).

Sources of precursor emissions in the troposphere include biofuel combustion, methane emitted from swamps and wetlands, lightning strikes, emission from soils, and combustion of fossil fuels [5]. Current models estimate that 30% of ozone formed from these precursor emissions are attributable to human activity [6] and that background mixing ratios have nearly doubled in the past 100 years [5]. Precursor emissions emitted through combustion of fossil fuels concentrates surface ozone in large urban areas. As such, high pollution events can affect an area as large as 600 square miles [7]. These types of events have been known to occur in the eastern U.S. and California. However, increased pollution is not limited to cities. Ozone precursors readily travel several hundred kilometers from urban regions [7]. This can cause increased ozone concentrations in areas far away and across oceans from emission centers.

Human health impacts are the primary motivation in reducing U.S. surface ozone levels. Inhalation of ozone can cause chest pain, throat irritation, airway inflammation, and reduce lung function [8]. In addition, it has a damaging effect on crops and vegetation [8], which can have an economic impact. As a result of these findings, National Ambient Air Quality Standards (NAAQS) are set for ozone by the United States Environmental Protection Agency (EPA) under the authority of the Clean Air Act of 1970 [9,10]. The NAAQS for ozone has changed periodically since then, with the most recent change to the standard occurring in 2015 when it was lowered from the 2008 level of 0.075 ppmv to 0.070 ppmv [11,12].

Given all the factors affecting ozone concentrations, setting and maintaining standards requires extensive examination and study. This document focuses on several of the drivers of variability in ozone concentrations using data from National Parks across the U.S. These are mostly remote areas without the influence of fresh anthropogenic emissions. We examine sites that are a part of the United States National Park Service Gaseous Pollutant Monitoring Program (U.S. NPS GPMP) using a data decomposition technique, the Ensemble Empirical Mode Decomposition (EEMD). Decomposing ozone data helps to better understand the factors driving ozone trends and variability. To do so, long-term ozone data were decomposed into long-term trends and seasonal, interannual, and interdecadal time-scales. First, long-term trends were quantified. The date the trends changed from positive to negative was determined, if present, then, each oscillatory component was analyzed in turn. Spatial and temporal variability for long-term trends and the seasonal cycle was determined. The seasonal cycle was examined further, where the effect of low frequency climate modes on this component was quantified. With this information, implications of the effect of lower frequency oscillatory components on higher frequency components were drawn.

1.1 References

1. IPCC *Climate Change 2014: Mitigation of Climate Change. Summary for Policymakers and Technical Summary*; 2014; ISBN 9781107415416.
2. US Department of Commerce, N. E. S. R. L. C. S. D. Scientific Assessment of Ozone Depletion 1994 - Common Questions About Ozone.
3. Chameides, W.; Walker, J. C. G. A photochemical theory of tropospheric ozone. *J. Geophys. Res.* **1973**, *78*, 8751–8760, doi:10.1029/JC078i036p08751.
4. Crutzen, P. J. Photochemical reactions initiated by and influencing ozone in unpolluted

tropospheric air. *Tellus* **1974**, *26*, 47–57, doi:10.1111/j.2153-3490.1974.tb01951.x.

5. Vingarzan, R. A review of surface ozone background levels and trends. *Atmos. Environ.* **2004**, *38*, 3431–3442, doi:10.1016/j.atmosenv.2004.03.030.

6. Cooper, O. R.; Parrish, D. D.; Ziemke, J.; Balashov, N. V.; Cupeiro, M.; Galbally, I. E.; Gilge, S.; Horowitz, L.; Jensen, N. R.; Lamarque, J.-F.; Naik, V.; Oltmans, S. J.; Schwab, J.; Shindell, D. T.; Thompson, A. M.; Thouret, V.; Wang, Y.; Zbinden, R. M. Global distribution and trends of tropospheric ozone: An observation-based review. *Elem. Sci. Anthr.* **2014**, *2*, doi:10.12952/journal.elementa.000029.

7. Sillman, S. The relation between ozone, NO(x) and hydrocarbons in urban and polluted rural environments. *Atmos. Environ.* **1999**, *33*, 1821–1845, doi:10.1016/S1352-2310(98)00345-8.

8. US Environmental Protection Agency *Overview of EPA's Updates to the Air Quality Standards for Ground-Level Ozone*; 2015;

9. EPA *Air Quality Criteria for Ozone and Related Photochemical Oxidants Volume I of III*; 2006; Vol. I;

10. US EPA Epa's 2015 ozone standard: concerns over science and implementation 2015, 1–354.

11. US Environmental Protection Agency *National ambient air quality standards for ozone; final rule-2008*; 2008; Vol. 73;.

12. US Environmental Protection Agency *National Ambient Air Quality Standard for Ozone; final Rule-2015*; 2015; Vol. 80;.

Chapter 2: Review of Current Literature

2.1 Tropospheric ozone

Tropospheric ozone (O_3), or ozone of the lowest layer of the atmosphere [1] forms through photochemical reactions of ozone precursor emissions with sunlight [2,3]. Ozone's precursor gases include methane (CH_4), carbon monoxide (CO), volatile organic compounds (VOCs), and nitrogen oxides (NO_x) [4,5]. Sources of precursor emissions include lightning (NO_x), soils (NO_x), wildfires, wetlands (CH_4), and anthropogenic emissions [4]. According to the EPA, 90% of NO_x emissions come from mobile, fuel combustion other than transportation, or industrial emissions and, the vast majority (90%) of fossil fuel combustion occurs in the Northern Hemisphere [4], resulting in rising surface ozone concentrations in this region [6]. In recent decades, ozone declined in the U.S., due to the implementation of air quality standards. However, decreasing concentrations have not been consistent across the country [6]. Ozone air quality standards in the western U.S. face challenges from increasing emissions in East Asia and the transport of these emissions to this region [6]. Therefore, careful assessment of ozone concentrations promises insight to further reduce surface ozone.

2.2 Formation and destruction of tropospheric ozone

Ozone forms through a set of complex chemical reactions, initiated by the oxidation of VOCs or carbon monoxide (CO) [7]. Reaction by either of these with a hydroxy radical ($^{\bullet}OH$) forms an intermediate radical which rapidly reacts with oxygen to form a peroxy radical ($HO_2^{\bullet}$ or $RO_2^{\bullet}$) (**R1** and **R2**) [7]. $HO_2^{\bullet}$ or $RO_2^{\bullet}$ goes on to react with nitric oxide ($^{\bullet}NO$) to yield nitrogen dioxide ($^{\bullet}NO_2$) (**R3**) [7]. Nitrogen dioxide is photolyzed at $\lambda < 424$ nm to yield atomic oxygen (**R4**) [7,8]. In the last step, atomic oxygen reacts with molecular oxygen to form ozone (**R5**).

Ozone formation initiated by reaction of CO with a hydroxy radical described in the above-mentioned steps, is illustrated in the reaction mechanism below [7,8]:

R1 $^{\bullet}OH + CO \rightarrow HOCO^{\bullet}$

R2 $HOCO^{\bullet} + O_2 \rightarrow HO_2^{\bullet} + CO_2$

R3 $HO_2^{\bullet} + {}^{\bullet}NO \rightarrow {}^{\bullet}OH + {}^{\bullet}NO_2$

R4 $^{\bullet}NO_2 + h\nu\ (\lambda < 424\ nm) \rightarrow {}^{\bullet}NO + O(^3P)$

R5 $O(^3P) + O_2 \rightarrow O_3$

Initiation of ozone formation starting with ethane is illustrated here:

R6 $CH_3CH_3 + {}^{\bullet}OH \rightarrow CH_3C^{\bullet}H_2 + H_2O$

R7 $CH_3CH_2^{\bullet} + O_2 \rightarrow CH_3CH_2OO^{\bullet}$

R8 $CH_3CH_2OO^{\bullet} + {}^{\bullet}NO_2 \leftrightarrow CH_3CH_2OONO_2$

R9 $CH_3CH_2OO^{\bullet} + {}^{\bullet}NO \rightarrow CH_3CH_2O^{\bullet} + {}^{\bullet}NO_2$

R10 $CH_3CH_2O^{\bullet} + O_2 \rightarrow CH_3CHO^{\bullet} + HO_2^{\bullet}$

R11 $HO_2^{\bullet} + {}^{\bullet}NO \rightarrow {}^{\bullet}OH + {}^{\bullet}NO_2$

R12 $^{\bullet}NO_2 + h\nu\ (\lambda < 424\ nm) \rightarrow {}^{\bullet}NO + O(^3P)$

R13 $O(^3P) + O_2 \rightarrow O_3$

The reaction mechanism above is initiated with ethane and a hydroxy radical (**R6**), rather than CO with a hydroxy radical [7,9]. Please note that R can represent any length of organic chain.

The steady-state Leighton relationship quantifies the amount of ozone produced in areas polluted with nitrogen oxides (NO_x) [8]. Through photolysis at wavelengths less than 424 nm, NO_x is the primary precursor species for ozone production, as seen in the last three reactions of the mechanisms illustrated above. This relationship also shows how the production of ozone is directly related to solar radiation intensity [8]. The mechanism determining the Leighton

relationship is listed below. These are also the last three reactions represented in the mechanisms previously discussed.

R14 $^{\bullet}NO_2 + h\nu\ (\lambda < 424\ nm) \rightarrow {}^{\bullet}NO + O(^3P)$ J_{14}

R15 $O\ (^3P) + O_2 + M \rightarrow O_3 + M$ k_{15}

R16 $O_3 + {}^{\bullet}NO \rightarrow {}^{\bullet}NO_2 + O_2$ k_{16}

The steady-state Leighton relationship is as follows [8]:

$$[O_3] = \frac{J_{14}[NO_2]}{k_{16}[NO]}$$

The primary loss process of tropospheric ozone is photolysis [8] and is shown here:

R17 $O_3 + h\nu\ (\lambda < 320\ nm) \rightarrow O_2 + O(^1D)$

In a NO_x – rich environment, ozone destruction will also follow this mechanism [8]:

R16 $O_3 + {}^{\bullet}NO \rightarrow O_2 + {}^{\bullet}NO_2$

In a NO_x – poor environment, ozone destruction will more likely follow this mechanism [8]:

R18 $CO + {}^{\bullet}OH \rightarrow H^{\bullet} + CO_2$

R19 $H^{\bullet} + O_2 + M \rightarrow HO_2{}^{\bullet} + M$

R20 $HO_2{}^{\bullet} + O_3 \rightarrow {}^{\bullet}OH + 2O_2$

Furthermore, ozone destruction can occur directly through a reaction with $^{\bullet}OH$:

R20 $^{\bullet}OH + O_3 \rightarrow HO_2{}^{\bullet} + 2O_2$

2.3 Health effects from elevated surface ozone

Ground-level ozone is the subject of many studies given its detrimental health effects [10,11]. At high concentrations, ozone causes irritation of the respiratory system resulting in chest and throat irritation [10,11]. This sensation is due to the inflammation to the lining of the lungs which reduces lung function and makes rigorous activities difficult [10,11]. An increased number of asthma attacks occur when ozone concentrations are high [12]. In addition, there is an

increased susceptibility to respiratory infections [10,11]. People that have the highest risk of having symptoms from high ozone include people with asthma, children and older adults, and people who regularly work outside [10,11]. When ozone concentrations rise above 50 ppbv, unusually sensitive groups are encouraged to reconsider long-term strenuous activities [12]. When ozone exceeds 100 ppbv, any persons that are at elevated risk such as those with asthma, the elderly, and children should reduce long-term outdoor activities [12]. Concentrations above 150 ppbv are unhealthy for all people for extended periods of time [12].

In addition to ozone's effect on human respiratory function, it also has adverse effects on vegetation. Ozone enters through gas exchange pores or stomata on plant leaves [13]. It then dissolves in water in the plant and reacts with other chemicals and fatty acids. Reactive oxygen species produced by this ozone interferes with the function of plant mitochondria [13]. This results in the slowing of photosynthesis which stunts plant growth and decreases the number of flowers and fruits produced by the plant [13]. Plants weakened by high concentrations of ozone are more susceptible to drought, pests, and disease [13].

2.4 Establishment of Environmental Protection Agency Ozone Standards

Given the health effects instigated by elevated levels of ozone, the United States Environmental Protection Agency (EPA) established National Ambient Air Quality Standards (NAAQS) under the authority of the Clean Air Act of 1970 [14]. For each of the six pollutants covered under the NAAQS, primary and secondary standards are set [15]. The primary standards are designed to protect human health while secondary standards protect crops, forests, and infrastructure [15]. For ozone, both the primary and secondary standards require that the annual fourth-highest daily maximum rolling 8-hour concentration, averaged over 3 years, remain below 0.070 ppmv [15]. When a new standard is set, within one year each state must submit an

assessment of all counties, indicating if the standard is met. Following this, the EPA will designate areas of the U.S. as either attainment or non-attainment areas, which is done within two years after a change to the standard [15]. At this time, there are approximately 300 counties in the United States that are designated as non-attainment areas, and they are typically within and around large urban areas [16].

2.5 Ozone Monitoring Network used in this study

The standards set by the EPA resulted in the establishment of a large network of monitoring sites. One such monitoring network is the National Park Service Gaseous Pollutant Monitoring Program (NPS GPMP) [17,18]. The NPS Air Resources Monitoring Division monitors air quality throughout the park system [18]. The network assesses air quality conditions and long-term trends in ozone, and other air pollutants that affect human health and vegetation [19]. Another primary use of these data is to check for compliance with the NAAQS for criteria air pollutants [19] such as ozone. All NPS data are collected by the NPS GPMP and accessed by its data access page: http://ard-request.air-resource.com/.

2.6 Background ozone, baseline ozone, and trends in surface ozone at different percentiles

NPS and several other monitoring networks aide in determining compliance with ozone standards and variability in trends. Studies focusing on ozone trends look for compliance within areas of non-attainment, as well as areas of well-mixed air, which are typically rural areas [20–25]. The 95^{th}, 50^{th}, and 5^{th} percentiles of ozone observations are frequently used to evaluate the status of ozone. The 95^{th} percentile identifies variation in the frequency of high ozone events, while variability in the 50^{th} percentile is indicative of changes in median ozone concentrations, and changes in the 5^{th} percentile are suggested to indicate changes in the inflow of baseline ozone [14].

In general, the eastern half of the U.S. has benefited more from emission reductions than the western half [14,21,24,25]. In the summer, ozone concentrations at the 95th percentile have dropped across the country, which is likely caused by regulations targeting NO_x concentrations [4,14,20,21,26]. Less significant summer decreases at the 95th percentile have occurred in the west due to the aforementioned influx of precursor emissions from East Asia. This influx has resulted in ozone concentration increases at the 5th and 50th percentiles in all seasons in the west [14]. In the winter, ozone concentrations have increased across the country at the 5th percentile due to decreases in NO_x concentrations. Ozone increases as a result of decreasing NO_x because it is destroyed by reaction with NO. Therefore, a decrease in NO results in an increase in O_3. Reaction **R16** in section 2.2 depicts this ozone loss mechanism [14,21].

The U.S. Environmental Protection Agency also reviews trends in Policy Relevant Background (PRB) ozone. PRB ozone is defined as concentrations that would occur in the U.S. in the absence of anthropogenic emissions in continental North America [27,28]. Background ozone in the U.S. includes the influence of Asian anthropogenic emissions and wildfire emissions, which is quantified with the use of atmospheric models [27]. These areas are more likely to exceed the standard given that these sources cannot be helped by US ozone standards. [21].

Baseline ozone is ozone that has not been influenced by recent, locally emitted, or produced pollution [29,30]. In recent years, baseline ozone has been rising [25,31], affecting ozone concentrations across the US. This is of concern in the spring and summer months when ozone concentrations are the highest, making it difficult to maintain standards during this time. In a recent study by Parrish et. al [29], one site in the western U.S. (LAVO-ML) is identified as having a reversal in baseline ozone trends. The trend changed from positive to negative in the

early to mid-2000s. This date varied for different seasons. Parrish et. al [29] also verified this for the North American Free Troposphere and the Pacific Marine Boundary Layer. This reversal is attributed to a decrease in the influx of baseline ozone. This is the first study to find that ozone trends have changed from increasing to decreasing. The authors also point out that model studies may be misrepresenting the state of baseline ozone trends [29].

2.7 The ozone seasonal cycle

The ozone seasonal cycle is characterized by annual spring/summer maxima and late fall/winter minima in the northern mid-latitudes [32–34]. Furthermore, the variance was found to be the largest at one site analyzed frequently for variability in the ozone seasonal cycle, Mace Head, Ireland [35]. This is likely the case at most sites in the northern mid-latitudes due to ozone's dependence on sunlight and temperature [33,35,36]. Additionally, the seasonal cycle is driven more by the varying levels of precursor emissions rather than by transport from the stratosphere [37,33]. At Mace Head, Ireland, the timing of peak ozone changed and the amplitude (between peak and minimum ozone) has increased between 1990 and 2004 by 0.18 ± 0.04 ppbv yr^{-1} [33,35,38].

Parrish et. al [36] and Cooper et. al [4] further analyzed the timing of annual ozone peaks. In these studies, a total of five sites in Europe and six sites in the US, all in the northern mid-latitudes, were analyzed. A total of five of the European and three of the US sites were found to have a significantly ($p<0.05$) earlier occurring peak by 1 to 3 months. These 5 studies indicate that the change in timing of peak ozone occurred largely because of decreasing summertime precursor emissions [4,36,38]. These studies also suggest that an increase in early spring and wintertime ozone result from less ozone lost by reaction with NO [39]. Other suggested causes include changes in atmospheric transport pathways, changes in transport from the stratosphere,

and factors related to climate change. The last-mentioned includes increasing temperature, variations in water vapor concentrations, or changes in natural emissions [36].

2.8 Effects of large-scale climate oscillations

Several large-scale climate oscillations are known to affect surface ozone concentrations [40]. Two such modes of variability include the El Niño Southern Oscillation (ENSO) and the Pacific Decadal Oscillation (PDO). Using the Geophysical Fluid Dynamic Laboratory Global Chemistry-Climate model (GFDL AM3), Lin et al. [40,41] found that ozone in the western U.S. is enhanced in the spring following an El Niño event. The same is true during a La Niña event for the Northwestern US. It is believed that ozone enhancements at these locations and phases of ENSO, are related to variability in the location of the subtropical and polar jet streams as a result of the atmospheric response to ENSO [40–43]. Lin et al. [41] also found that the PDO phase shift from warm to cold between 1998 and 1999 directed the flow of ozone-rich air from East Asia to the northwestern U.S. In addition, Newman et al. [44] and Wang et al. [45] found that ENSO is more likely to be in the El Niño state when PDO is positive and in the La Niña state when PDO is negative.

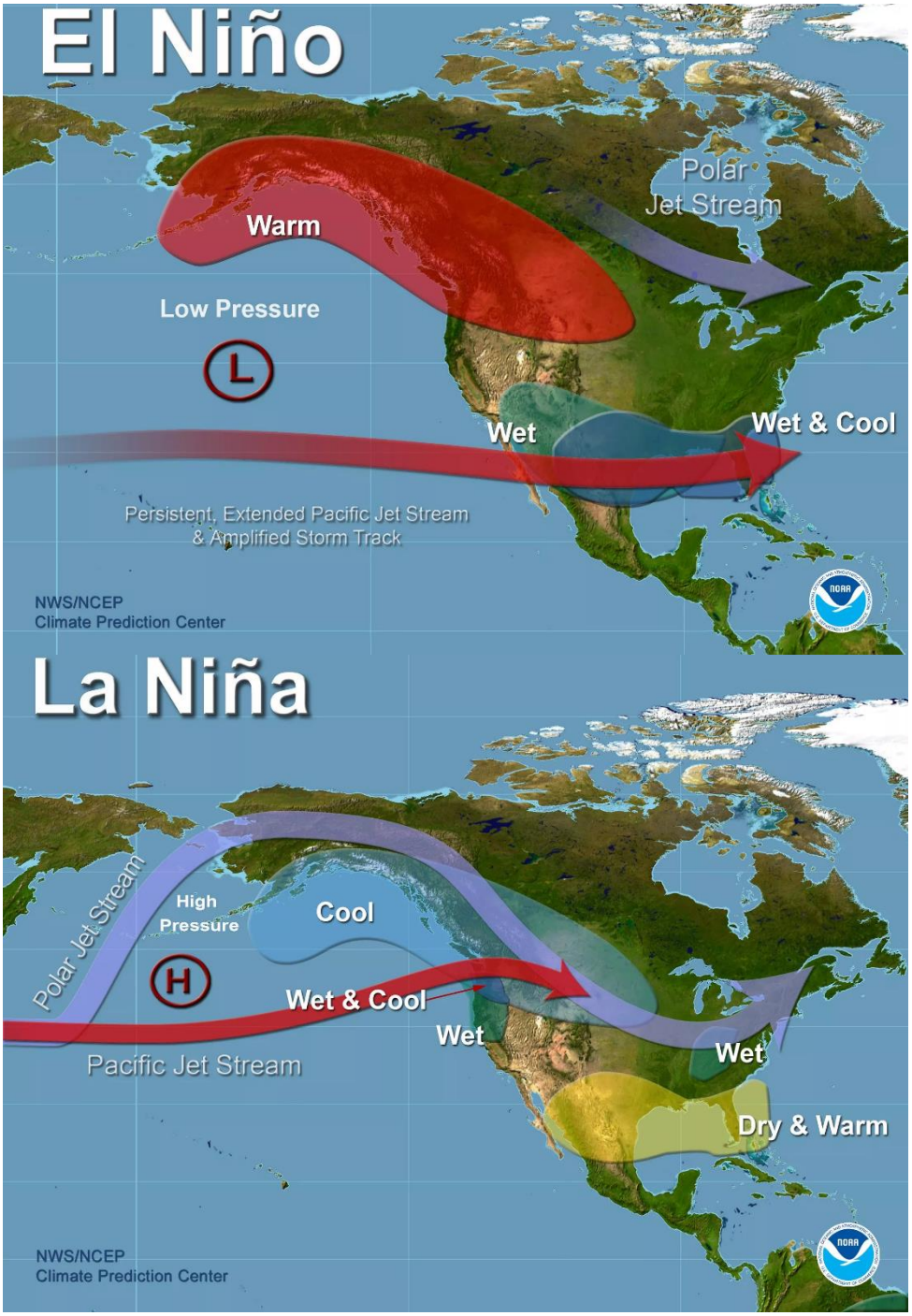

Figure 2.1: Teleconnections and location of the pacific (subtropical) and polar jet streams during El Niño (a) and La Niña (b). This figure was adapted from the National Oceanic and Atmospheric Administration [46].

Figure 2.1 depicts how transport of pollutants varies during the two phases of ENSO. When ENSO is in the El Niño phase, the subtropical jet stream is strengthened across the southern U.S. At this time, quick transport of pollutants from East Asia enhances ozone concentrations to this region (Figure 2.1 (a)) [40,41,46]. Weakening of the polar jet stream also occurs during El Niño. The subtropical jet weakens when ENSO is in the La Niña state but the flow of ozone-rich air from East Asia is directed to the Northwestern U.S. The polar jet stream is directed to latitudes above Alaska during La Niña (Figure 2.1 (b)) due to a high-pressure zone southwest of Alaska.

As previously mentioned, PDO influences the state and strength of ENSO. PDO is considered to be a long-lived, ENSO-type pattern of North Pacific climate variability on interdecadal timescales [44]. Figure 2.2 (a), depicts the cold phase of the PDO, presenting as a horseshoe type pattern along the western US and Aleutian Islands [47]. Cool sea surface

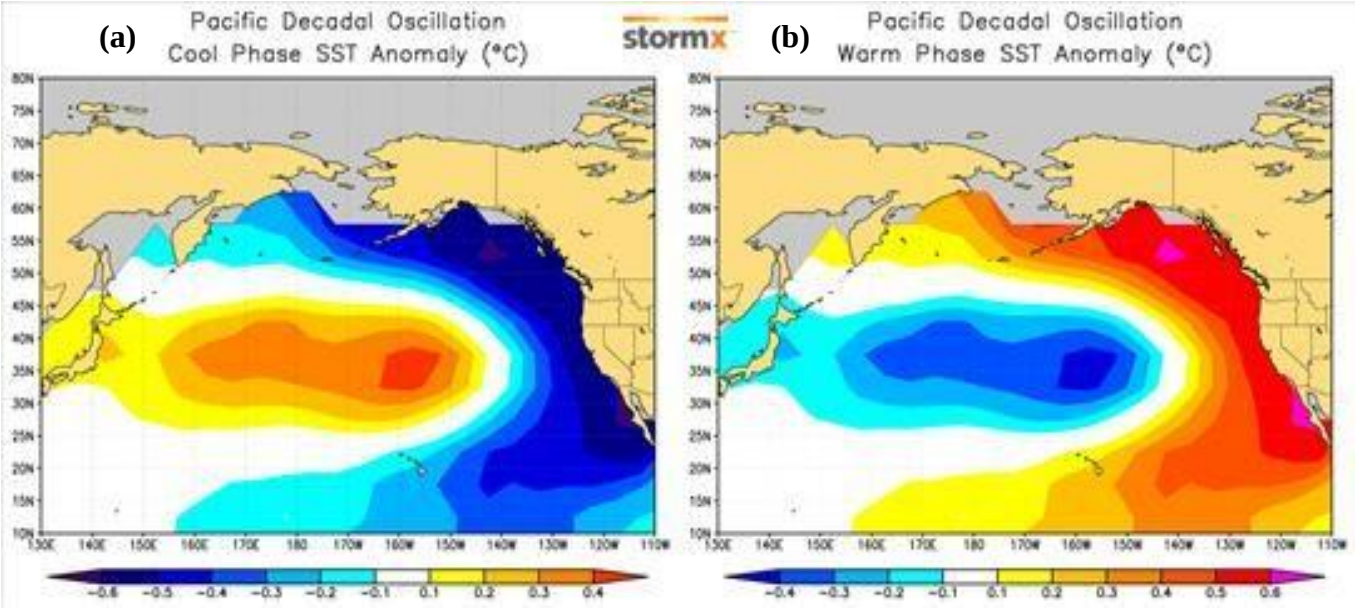

Figure 2.2: Surface skin anomalies in the North Pacific Ocean during a cold PDO (a) and a warm PDO (b) (adapted from Ross 2009) [47].

temperature (SST) anomalies occur along the coast while a warm SST anomaly occur throughout the middle of the North Pacific between the East Asian continent and North America [44]. The opposite occurs during a warm phase PDO, as shown in Figure 2.2 (b) [47].

2.9 Methods for analyzing data on different timescales

A frequency modulated time-series decomposition method, the Ensemble Empirical Mode Decomposition (EEMD), [48] is an algorithm that decomposes a time series into the temporal signals that make up the variability in a data set. The EEMD method introduces white noise of finite amplitude to the data set. This allows for components to be extracted in a thorough and finite manner and makes components distinguishable when sifting [48]. One issue is that the first couple of components do not always have a statistically significant difference from white noise [49].

EEMD splits a time series into k oscillatory components where components of higher frequency are extracted first [48]. The oscillatory components or signals are referred to as Intrinsic Mode Functions (IMFs) [48]. The number of IMFs of a data set are estimated to be $\log_2(N-1)$ [48,49], where N is the number of data points. Component IMFs obey two properties, (i) the number of local maxima and minima differ at most by 1 and (ii) an IMF has a mean value of zero [48,49]. The sifting process repeats until the mean of the signal is sufficiently close to zero. After all signals are extracted from the time series, the residual (R_n) of the raw data remains [48].

The use of this method is more economical than methods used in other studies. For example, trend analyses and the effect of climate on ozone concentrations require different methods for analyses. Ordinary Linear Regression (OLR) and Theil-Sen estimation is used for mean and quantile trend assessments while climate models are the only way of assessing trends

in background ozone. These methods do not allow for determination of how the trend of a data set has changed with time. A few methods are used in the extraction of ozone seasonal cycles. These include sinusoidal curve fitting to determine variability in the timing of peaks and troughs [36] and applying a simpler data decomposition technique to pull out seasonal variability and trends [35]. Global chemistry-climate models are used to assess background ozone trends and to determine the effect of large-scale climate patterns on wind, temperature, and pressure pattern changes [40,41]. Lin et al. [21,40,41] frequently use a Global Fluid Dynamic Model to quantify the effect of climate modes on ozone. However, the use of models can sometimes misestimate these effects. Therefore, it is important to use observational data to validate the findings from models.

In the past, detecting low frequency climate oscillations in a data set was difficult. However, this is now feasible with the Ensemble Empirical Mode Decomposition (EEMD) [48] which has been applied in several climate studies [50–55]. In each of these studies, the variability on timescales of days to several decades is elucidated from a data series. In some cases, interannual and multidecadal variability from the Atlantic Multidecadal Oscillation [50,51], the El Niño Southern Oscillation [54,55], the North Atlantic Oscillation [54], and long-term trends are identified and analyzed for variability or their effect on higher frequency components, such as the seasonal cycle [53]. In this work, this method was employed for determining changing surface ozone trends, ozone seasonal cycle variability, and the effects of large-scale climate oscillations on higher frequency components. It is also the first study to apply EEMD in ozone analysis.

In this study, ozone observations were taken from a multitude of National Park Service sites, some of which had never been analyzed. The sites across the U.S. National Parks had at

least 10 years of data, which could provide for a robust spatial and temporal analysis of ozone variability. Of these sites, only six had been analyzed for variability in the seasonal cycle in the U.S. In addition, worldwide, only 5 studies focused on variability in the seasonal cycle of ozone [4,33,35,36,38]. This was the first study to assess the effect of large-scale climate perturbations on ozone observations and to quantitatively determine the time-varying trend in surface ozone [29]. Understanding changes in the seasonal cycle, the effect of climate modes on ozone concentrations, and where emissions reductions have been effective can assist policy makers. This information can be used as solid scientific input for developing ozone mitigation strategies.

It is also important to determine how ozone levels have changed in the National Parks because many of these areas are Class 1 protected areas [56]. A Class 1 protected area is a geographic region recognized by the EPA as being of highest environmental quality [56]. Therefore, it is important to assess the state of environmental pollutants and determine if significant deleterious change has occurred [10,11].

2.10 References

1. Stevenson, D. S.; Dentener, F. J.; Schultz, M. G.; Ellingsen, K.; van Noije, T. P. C.; Wild, O.; Zeng, G.; Amann, M.; Atherton, C. S.; Bell, N.; Bergmann, D. J.; Bey, I.; Butler, T.; Cofala, J.; Collins, W. J.; Derwent, R. G.; Doherty, R. M.; Drevet, J.; Eskes, H. J.; Fiore, A. M.; Gauss, M.; Hauglustaine, D. A.; Horowitz, L. W.; Isaksen, I. S. A.; Krol, M. C.; Lamarque, J.-F.; Lawrence, M. G.; Montanaro, V.; Müller, J.-F.; Pitari, G.; Prather, M. J.; Pyle, J. A.; Rast, S.; Rodriguez, J. M.; Sanderson, M. G.; Savage, N. H.; Shindell, D. T.; Strahan, S. E.; Sudo, K.; Szopa, S. Multimodel ensemble simulations of present-day and near-future tropospheric ozone. *J. Geophys. Res.* **2006**, *111*, D08301, doi:10.1029/2005JD006338.

2. Stohl, A. Stratosphere-troposphere exchange: A review, and what we have learned from STACCATO. *J. Geophys. Res.* **2003**, *108*, 8516, doi:10.1029/2002JD002490.

3. Junge, C. E. Global ozone budget and exchange between stratosphere and troposphere. *Tellus* **1962**, *14*, 363–377, doi:10.3402/tellusa.v14i4.9563.

4. Cooper, O. R.; Parrish, D. D.; Ziemke, J.; Balashov, N. V.; Cupeiro, M.; Galbally, I. E.; Gilge, S.; Horowitz, L.; Jensen, N. R.; Lamarque, J.-F.; Naik, V.; Oltmans, S. J.; Schwab, J.; Shindell, D. T.; Thompson, A. M.; Thouret, V.; Wang, Y.; Zbinden, R. M. Global distribution and trends of tropospheric ozone: An observation-based review. *Elem. Sci. Anthr.* **2014**, *2*, doi:10.12952/journal.elementa.000029.

5. Monks, P. S.; Granier, C.; Fuzzi, S.; Stohl, A.; Williams, M. L.; Akimoto, H.; Amann, M.; Baklanov, A.; Baltensperger, U.; Bey, I.; Blake, N.; Blake, R. S.; Carslaw, K.; Cooper, O. R.; Dentener, F.; Fowler, D.; Fragkou, E.; Frost, G. J.; Generoso, S.; Ginoux, P.; Grewe, V.; Guenther, A.; Hansson, H. C.; Henne, S.; Hjorth, J.; Hofzumahaus, A.; Huntrieser, H.; Isaksen, I. S. A.; Jenkin, M. E.; Kaiser, J.; Kanakidou, M.; Klimont, Z.; Kulmala, M.; Laj, P.; Lawrence, M. G.; Lee, J. D.; Liousse, C.; Maione, M.; McFiggans, G.; Metzger, A.; Mieville, A.; Moussiopoulos, N.; Orlando, J. J.; O'Dowd, C. D.; Palmer, P. I.; Parrish, D. D.; Petzold, A.; Platt, U.; Pöschl, U.; Prévôt, A. S. H.; Reeves, C. E.; Reimann, S.; Rudich, Y.; Sellegri, K.; Steinbrecher, R.; Simpson, D.; ten Brink, H.; Theloke, J.; van der Werf, G. R.; Vautard, R.; Vestreng, V.; Vlachokostas, C.; von Glasow, R. Atmospheric composition change – global and regional air quality. *Atmos. Environ.* **2009**, *43*, 5268–5350, doi:10.1016/j.atmosenv.2009.08.021.

6. Dentener, F., Keating, T., Akimoto, H. *Hemispheric Transport of 2010 Part A: Ozone and*

Particulate Matter; United Nations Publication: Geneva, 2010; ISBN 978-92-1-117043-6.

7. Sillman, S. *Overview: tropospheric ozone, smog and ozone-NOx-VOC sensitivity*; 2003;

8. Seinfeld, JH; Pandis, S. *Atmospheric Chemistry and Physics: from Air Pollution to Climate Change*; second.; Wiley, 2006; Vol. 52; ISBN 9780471720171.

9. Seinfeld, J. H.; Pandis, S. N. *ATMOSPHERIC From Air Pollution to Climate Change SECOND EDITION*; 2006; ISBN 9780471720171.

10. US Environmental Protection Agency *National Ambient Air Quality Standard for Ozone; final Rule-2015*; 2015; Vol. 80;.

11. US Environmental Protection Agency *National ambient air quality standards for ozone; final rule-2008*; 2008; Vol. 73;.

12. U.S. EPA Air Quality Guide for Ozone Available online: https://www.airnow.gov/index.cfm?action=pubs.aqiguideozone (accessed on Apr 24, 2018).

13. Kangasjarvi, J.; Jaspers, P.; Kollist, H. Signalling and cell death in ozone-exposed plants. *Plant, Cell Environ.* **2005**, *28*, 1021–1036, doi:10.1111/j.1365-3040.2005.01325.x.

14. Cooper, O. R.; Gao, R. S.; Tarasick, D.; Leblanc, T.; Sweeney, C. Long-term ozone trends at rural ozone monitoring sites across the United States, 1990-2010. *J. Geophys. Res. Atmos.* **2012**, *117*, D22307, doi:10.1029/2012JD018261.

15. US Environmental Protection Agency *Overview of EPA's Updates to the Air Quality Standards for Ground-Level Ozone*; 2015;

16. US EPA Epa's 2015 ozone standard: concerns over science and implementation 2015, 1–

354.

17. National Park Service Ozone and Meteorology Monitoring Available online: https://www.nature.nps.gov/air/monitoring/network.cfm (accessed on Mar 10, 2018).

18. National Park Service Air Resources Division *Gaseous Pollutant Monitoring Program Quality Assurance Project Plan (QAPP)*; 2015;

19. U.S. Department of the Interior National Park Service *Air Quality in National Parks, 2008 Annual Performance & Progress Report*; 2010;

20. Cooper, O. R. Trends in northern hemisphere ozone since the 1970s and the rise in baseline ozone observed across western North America Background vs Baseline ozone. **2015**, 1–37.

21. Lin, M.; Horowitz, L. W.; Payton, R.; Fiore, A. M.; Tonnesen, G. US surface ozone trends and extremes from 1980 to 2014: quantifying the roles of rising Asian emissions, domestic controls, wildfires, and climate. *Atmos. Chem. Phys.* **2017**, *17*, 2943–2970, doi:10.5194/acp-17-2943-2017.

22. Jaffe, D.; Ray, J. Increase in surface ozone at rural sites in the western US. *Atmos. Environ.* **2007**, *41*, 5452–5463, doi:10.1016/j.atmosenv.2007.02.034.

23. Lefohn, A. S.; Shadwick, D.; Oltmans, S. J. Characterizing changes in surface ozone levels in metropolitan and rural areas in the United States for 1980–2008 and 1994–2008. *Atmos. Environ.* **2010**, *44*, 5199–5210, doi:10.1016/j.atmosenv.2010.08.049.

24. Oltmans, S. J.; Lefohn, A. S.; Harris, J. M.; Galbally, I.; Scheel, H. E.; Bodeker, G.; Brunke, E.; Claude, H.; Tarasick, D.; Johnson, B. J.; Simmonds, P.; Shadwick, D.; Anlauf,

K.; Hayden, K.; Schmidlin, F.; Fujimoto, T.; Akagi, K.; Meyer, C.; Nichol, S.; Davies, J.; Redondas, A.; Cuevas, E. Long-term changes in tropospheric ozone. *Atmos. Environ.* **2006**, *40*, 3156–3173, doi:10.1016/j.atmosenv.2006.01.029.

25. Parrish, D. D.; Law, K. S.; Staehelin, J.; Derwent, R.; Cooper, O. R.; Tanimoto, H.; Volz-Thomas, A.; Gilge, S.; Scheel, H.-E.; Steinbacher, M.; Chan, E. Long-term changes in lower tropospheric baseline ozone concentrations at northern mid-latitudes. *Atmos. Chem. Phys.* **2012**, *12*, 11485–11504, doi:10.5194/acp-12-11485-2012.

26. Simon, H.; Reff, A.; Wells, B.; Xing, J.; Frank, N. Ozone trends across the United States over a period of decreasing NOx and VOC emissions. *Environ. Sci. Technol.* **2015**, *49*, 186–195, doi:10.1021/es504514z.

27. McDonald-Buller, E. C.; Allen, D. T.; Brown, N.; Jacob, D. J.; Jaffe, D.; Kolb, C. E.; Lefohn, A. S.; Oltmans, S.; Parrish, D. D.; Yarwood, G.; Zhang, L. Establishing Policy Relevant Background (PRB) Ozone Concentrations in the United States. *Environ. Sci. Technol.* **2011**, *45*, 9484–9497, doi:10.1021/es2022818.

28. US Environmental Protection Agency *Policy Assessment for the Review of the Ozone National Ambient Air Quality Standards*; 2014;

29. Parrish, D. D.; Petropavlovskikh, I.; Oltmans, S. J. Reversal of Long-Term Trend in Baseline Ozone Concentrations at the North American West Coast. *Geophys. Res. Lett.* **2017**, *44*, 10,675-10,681, doi:10.1002/2017GL074960.

30. D.D. Parrish et. al. Long-term changes in lower tropospheric baseline ozone concentrations: Comparing chemistry-climate models and observations at northern midlatitudes. *J. Geophys. Res. Atmos.* **2014**, *119*, 5719–5736,

doi:10.1002/2013JD021060.Received.

31. Baylon, P. M.; Jaffe, D. A.; Pierce, R. B.; Gustin, M. S. Interannual Variability in Baseline Ozone and Its Relationship to Surface Ozone in the Western U.S. *Environ. Sci. Technol.* **2016**, *50*, 2994–3001, doi:10.1021/acs.est.6b00219.

32. Derwent, R. G.; Jenkin, M. E.; Saunders, S. M.; Pilling, M. J. Photochemical ozone creation potentials for organic compounds in northwest Europe calculated with a master chemical mechanism. *Atmos. Environ.* **1998**, *32*, 2429–2441, doi:10.1016/S1352-2310(98)00053-3.

33. Monks, P. S. A review of the observations and origins of the spring ozone maximum. *Atmos. Environ.* **2000**, *34*, 3545–3561, doi:10.1016/S1352-2310(00)00129-1.

34. Wang, Y. Springtime photochemistry at northern mid and high latitudes. *J. Geophys. Res.* **2003**, *108*, 8358–8390, doi:10.1029/2002JD002227.

35. Carslaw, D. C. On the changing seasonal cycles and trends of ozone at Mace Head, Ireland. *Atmos. Chem. Phys. Discuss.* **2005**, *5*, 5987–6011, doi:10.5194/acpd-5-5987-2005.

36. Parrish, D. D.; Law, K. S.; Staehelin, J.; Derwent, R.; Cooper, O. R.; Tanimoto, H.; Volz-Thomas, A.; Gilge, S.; Scheel, H.-E.; Steinbacher, M.; Chan, E. Lower tropospheric ozone at northern midlatitudes: Changing seasonal cycle. *Geophys. Res. Lett.* **2013**, *40*, 1631–1636, doi:10.1002/grl.50303.

37. Chameides, W.; Walker, J. C. G. A photochemical theory of tropospheric ozone. *J. Geophys. Res.* **1973**, *78*, 8751–8760, doi:10.1029/JC078i036p08751.

38. Salisbury, G.; Monks, P. S.; Bauguitte, S.; Bandy, B. J.; Penkett, S. A. A Seasonal Comparison of the Ozone Photochemistry in Clean and Polluted Air Masses at Mace Head, Ireland. *J. Atmos. Chem.* **2002**, *41*, 163–187, doi:10.1023/A:1014202229304.

39. Jonson, J. E.; Simpson, D.; Fagerli, H.; Solberg, S. Can we explain the trends in European ozone levels? *Atmos. Chem. Phys.* **2006**, *6*, 51–66, doi:10.5194/acp-6-51-2006.

40. Lin, M.; Fiore, A. M.; Horowitz, L. W.; Langford, A. O.; Oltmans, S. J.; Tarasick, D.; Rieder, H. E. Climate variability modulates western US ozone air quality in spring via deep stratospheric intrusions. *Nat. Commun.* **2015**, *6*, 7105–7116, doi:10.1038/ncomms8105.

41. Lin, M.; Horowitz, L. W.; Oltmans, S. J.; Fiore, A. M.; Fan, S. Tropospheric ozone trends at Mauna Loa Observatory tied to decadal climate variability. *Nat. Geosci.* **2014**, *7*, 136–143, doi:10.1038/ngeo2066.

42. Chandra, S.; Ziemke, J. R.; Min, W.; Read, W. G. Effects of 1997-1998 El Niño on tropospheric ozone and water vapor. *Geophys. Res. Lett.* **1998**, *25*, 3867–3870, doi:10.1029/98GL02695.

43. Oman, L. D.; Ziemke, J. R.; Douglass, A. R.; Waugh, D. W.; Lang, C.; Rodriguez, J. M.; Nielsen, J. E. The response of tropical tropospheric ozone to ENSO. *Geophys. Res. Lett.* **2011**, *38*, L13706, doi:10.1029/2011GL047865.

44. Newman, M.; Compo, G. P.; Alexander, M. A. ENSO-Forced Variability of the Pacific Decadal Oscillation. *J. Clim.* **2003**, *16*, 3853–3857, doi:10.1175/1520-0442(2003)016<3853:EVOTPD>2.0.CO;2.

45. Wang, H.; Kumar, A.; Wang, W.; Xue, Y. Seasonality of the Pacific Decadal Oscillation. *J. Clim.* **2012**, *25*, 25–38, doi:10.1175/2011JCLI4092.1.

46. NOAA NOAA: La Niña ends, increasing odds El Niño will return winter 2017-2018 Available online: https://addins.wpta21.com/blogs/weather/noaa-la-nina-ends-increasing-odds-el-nino-will-return-winter-2017-2018/ (accessed on Mar 20, 2018).

47. Ross, J. The Pacific Ocean's Influence on Climate Change: How Low Will the PDO Go? Available online: https://www.sott.net/article/183250-The-Pacific-Oceans-Influence-on-Climate-Change-How-Low-Will-the-PDO-Go (accessed on Mar 20, 2018).

48. Wu and Huang Ensemble Empirical Mode Decomposition: A Noise Assisted Data Analysis Method. *Adv. Adapt. Data Anal.* **2009**, *1*, 385–388.

49. Wu, Z.; Huang, N. E.; Long, S. R.; Peng, C.-K. On the trend, detrending, and variability of nonlinear and nonstationary time series. *Proc. Natl. Acad. Sci.* **2007**, *104*, 14889–14894, doi:10.1073/pnas.0701020104.

50. Fu, C.; Qian, C.; Wu, Z. Projection of global mean surface air temperature changes in next 40 years: Uncertainties of climate models and an alternative approach. *Sci. China Earth Sci.* **2011**, *54*, 1400–1406, doi:10.1007/s11430-011-4235-9.

51. Wu, Z.; Huang, N. E.; Wallace, J. M.; Smoliak, B. V.; Chen, X. On the time-varying trend in global-mean surface temperature. *Clim. Dyn.* **2011**, *37*, 759–773, doi:10.1007/s00382-011-1128-8.

52. Ji, F.; Wu, Z.; Huang, J.; Chassignet, E. P. Evolution of land surface air temperature trend. *Nat. Clim. Chang.* **2014**, *4*, 462–466, doi:10.1038/nclimate2223.

53. Wu, Z.; Schneider, E. K.; Kirtman, B. P.; Sarachik, E. S.; Huang, N. E.; Tucker, C. J. The modulated annual cycle: an alternative reference frame for climate anomalies. *Clim. Dyn.* **2008**, *31*, 823–841, doi:10.1007/s00382-008-0437-z.

54. Guo, B.; Chen, Z.; Guo, J.; Liu, F.; Chen, C.; Liu, K. Analysis of the Nonlinear Trends and Non-Stationary Oscillations of Regional Precipitation in Xinjiang, Northwestern China, Using Ensemble Empirical Mode Decomposition. *Int. J. Environ. Res. Public Health* **2016**, *13*, 345–365, doi:10.3390/ijerph13030345.

55. Zhang, A.; Jia, G.; Epstein, H. E.; Xia, J. ENSO elicits opposing responses of semi-arid vegetation between Hemispheres. *Sci. Rep.* **2017**, *7*, 42281–42290, doi:10.1038/srep42281.

56. US Environmental Protection Agency Class 1 Areas - Data.gov Available online: https://catalog.data.gov/dataset/class-1-areas (accessed on Feb 1, 2018).

Chapter 3: Understanding long-term variations in surface ozone in United States (U.S.) National Parks

Abstract

Long-term surface ozone observations at 25 National Park Service sites across the United States were analyzed for processes on varying time scales using a time scale decomposition technique, the Ensemble Empirical Mode Decomposition (EEMD). Time scales of interest include the seasonal cycle, large-scale climate oscillations, and long-term (>10 years) trends. Emission reductions were found to have a greater impact on sites that are nearest major urban areas. Multidecadal trends in surface ozone were increasing at a rate of 0.07 to 0.37 ppbv $year^{-1}$ before 2004 and decreasing at a rate of −0.08 to −0.60 ppbv $year^{-1}$ after 2004 for sites in the East, Southern California, and Northwestern Washington. Sites in the Intermountain West did not experience a reversal of trends from positive to negative until the mid- to late 2000s. The magnitude of the annual amplitude (=annual maximum–minimum) decreased at eight sites, two in the West, two in the Intermountain West, and four in the East, by 5–20 ppbv and significantly increased at three sites; one in Alaska, one in the West, and one in the Intermountain West, by 3–4 ppbv. Stronger decreases in the annual amplitude occurred at a greater proportion of sites in the East (4/6 sites) than in the West/Intermountain West (4/19 sites). The date of annual maximums and/or minimums has changed at 12 sites, occurring 10–60 days earlier in the year. There appeared to be a link between the timing of the annual maximum and the decrease in the annual amplitude, which was hypothesized to be related to a decrease in ozone titration resulting from NO_x emission reductions. Furthermore, it was found that a phase shift of the Pacific Decadal Oscillation (PDO), from positive to negative, in 1998–1999 resulted in increased occurrences of La Niña-like conditions. This shift had the effect of directing more polluted air masses from East Asia to higher latitudes of the North American continent. The change in the Pacific Decadal Oscillation (PDO)/El Niño Southern Oscillation (ENSO) regime influenced surface ozone at an Alaskan site over its nearly 30-year data record.

Keywords: ozone; trends; Ensemble Empirical Mode Decomposition; annual amplitude; seasonal cycle; El Niño Southern Oscillation; Pacific Decadal Oscillation; National Park Service

3.1 Introduction

High concentrations of tropospheric ozone can have adverse effects on human health and vegetation. The United States (U.S.) Environmental Protection Agency (EPA) recently lowered the National Ambient Air Quality Standard (NAAQS) for ozone from 75 ppbv to 70 ppbv [1,2], in 2015. To attain the ozone NAAQS, a monitor's fourth-highest annual daily maximum 8-h average ozone concentration (DM8HA) averaged over three consecutive years (i.e., the monitor's design value) must not exceed 70 ppbv [1,2]. Regional emission controls for nitrogen oxides (NO_x) have aided in the decrease of summertime ozone in the eastern U.S. as well as parts of California [3,4]. There are concerns that the influx of East Asian emissions [4–6], and the influences by interannual and interdecadal variability in the El Niño Southern Oscillation (ENSO) and the Pacific Decadal Oscillation (PDO) may make ozone attainment difficult for regions of higher elevation in the western U.S. [5,7–9]. Meeting and maintaining lower ozone standards may also be more difficult in a warming climate [11]. A quantitative understanding of the spatiotemporal variability in observed ozone on time scales of days to decades can assist policy makers in developing effective mitigation strategies for ozone abatement.

Regional U.S. ozone control strategies have successfully decreased DM8HA ozone in the eastern U.S., California, and the Intermountain West at the 95^{th}, 50^{th}, and 5^{th} percentiles in the summer months [7]. Similar decreases in the DM8HA ozone was found in spring, at the 95^{th} and 50^{th} percentile, but at fewer sites across the U.S. [7,9]. However, increases at the 5^{th} percentile were observed in most regions in springtime [7,9]. Recently, a leveling of the mean trend, followed by a slight decrease has been observed in the Pacific Northwest [12]. In addition to these observed changes, model simulations indicated that the springtime transport of East Asian pollution enhanced surface ozone at western U.S. sites by about 5 ppbv [13,14] and by up to 8–

15 ppbv during high pollution episodes [14]. Transport of ozone precursors from East Asia may be linked to increases in springtime ozone concentrations in portions of the western U.S. However, the transport of East Asian emissions varies with the transport pathway that is facilitated by large-scale circulation patterns, which may affect ozone concentrations on time scales of days to decades [7,8].

The effect of ENSO and PDO on ozone has been identified previously in both model and observation-based studies. ENSO and PDO influenced the origin and fate of air masses that are arriving to the U.S. [10,15]. Using an observation-based approach, Langford et al. [16] found that the effect of ENSO on ozone was largely dependent on the strength of the ENSO event in the Western U.S., and that ozone was anticorrelated with the Southern Oscillation Index (SOI). While using a model based approach, Koumoutsaris et al. [17] and Lin et al. [8] found that ozone transported to the northern mid-latitudes was enhanced in spring following an El Niño event and diminished following a La Niña event. Lin et al. [8] also suggested that transpacific transport of East Asian emissions to the western U.S. decreased after 1998 following a shift in the PDO phase from positive to negative. The negative phase of PDO is concurrent with a La Niña event, which shifts the subtropical jet stream to the north, thereby weakening transport of ozone-rich air from East Asia to the central west coast of the U.S., subsequently decreasing the transport of East Asian pollutants across the southern U.S. [8]. During peak La Niña periods, ozone-rich air was preferentially transported to the Pacific Northwest, thereby enhancing ozone concentrations to this area [8]. The peak phases of these climate modes potentially altered the timing, frequency, and magnitude of pollutant influx entering the western U.S. This, as well as regional ozone control standards, is believed to have played a role in the timing and magnitude of maximums and minimums of the seasonal ozone cycle across the northern mid-latitudes [18–20]. The effect

of these large-scale climate processes on surface ozone has yet to be sufficiently investigated and quantified using observation-based approaches.

Tropospheric ozone records show a pronounced seasonal cycle with peaks in late spring to summer and minimums in late fall to winter, which is largely driven by the photochemical production of ozone and temperature [21,22]. Monitoring sites in and around urban areas tend to have a mid-summer ozone peak resulting from maximum photochemical production during this season [23]. On the other hand, some high-elevation remote regions experience a late spring ozone maximum that is associated with stratospheric intrusions and hemisphere-wide photochemical production at this time of year [18–20]. Significant increases in springtime free tropospheric ozone over North America have been thought to largely result from the transport of polluted air masses from East Asia [9,24]. In addition, decreasing NO_x emissions in the northern mid-latitudes of Europe have resulted in less ozone titration by NO in early spring, further leading to a shift in the ozone annual maximum to earlier in the year [18,25]. At five sites in Europe and North America, peaks in the ozone seasonal cycle have shifted earlier by three to six days per decade; this trend was explained by changes in atmospheric dynamics, which may have aided in the change in distribution of precursor emissions throughout the year. Increased westerly flow related to changes in the North Atlantic Oscillation (NAO) in the 1980s and 1990s may have increased pollution levels and subsequently, ozone in the spring and winter months across the northern mid-latitudes [18]. Cooper et al. [26] focused on 8 sites between the U.S. and Europe, and found that between 1990 and 2010, five sites had peak ozone occurring 1–3 months earlier in the year. A systematic study is needed to understand how various long-term processes impact ozone on multiple timescales across the U.S. by using remote sites over the entire period of availability of ozone data sets.

Therefore, this study focuses on ozone trends from National Park Service sites as the remote locations of many of these sites are ideal for studying the long-term variation in surface ozone. Here, we examine ozone observations between 1983 and 2015 at 25 National Park sites that are operated by the U.S. National Park Service (NPS). The Ensemble Empirical Mode Decomposition (EEMD) method [27] was employed to analyze ozone on multiple temporal scales. When compared to other data analysis methods that are commonly used in the literature, EEMD is unique in its nonlinear trend assessment and more economic computing time.

3.2 Data and Methods

Daily data averaged from hourly data, collected by the NPS Gaseous Pollutant Monitoring Program (NPS GPMP), was used in this study (http://ard-request.air-resource.com/) [28]. Ozone is the primary gas monitored throughout the network that follows all EPA protocols and that is certified annually by the NPS to the EPA. The certification is supported by the Quality Assurance Project Plan (QAPP) [29], which specifically addresses the procedures used by the NPS to operate and certify ozone measurements at NPS-operated sites with EPA-certified analyzers. The data sets used here were all acquired from regulatory ozone monitoring stations; the sampling methods for gaseous and meteorological monitoring are based on the 40 CFR Part 58 requirements. All GPMP ambient ozone data is processed through several layers of rigorous validation by staff analysts. To ensure that each GPMP site and ozone monitor is operating properly and calibrated correctly, the full suite of GPMP network data are reviewed daily by a different independent analyst [29]. All data analysts follow the same quality assurance/quality control (QA/QC) protocols that are set by the QAPP [29]. Data analysts also monitor the amount of valid data acquired from each site and compare it to the expected amount under normal conditions in order to assess that data completeness criteria requirements are met or to

immediately identify a problem at a site. Additionally, the comparability of the data sets is monitored to ensure all final validated data is meaningfully comparable. Data validation for the entire GPMP network is performed monthly and uploaded to the EPA Air Quality System (AQS) database and is made available on the NPS Data Request web page. Further details regarding site operation and data processing can be found in the GPMP QAPP [29].

To study the variability of ozone on decadal to interdecadal time scales, all of the data sets used in this work had a minimum length of ten years. The locations and information for each site can be found in Table 3.1 and Figure 3.1. A total of 25 sites were available for this study which span time periods over 1983–2015. Of the sites used, six sites are in the eastern U.S., 18 are in the West and Intermountain West, and one is in Alaska. All of the sites are effectively far from urban centers and are representative of a well-mixed atmosphere [9]. Please note that the data series for ROMO-LP, in Colorado, started in 1987 however, between 1987 and 1997, 39% of the data during this period was missing. After this period, incomplete data dropped dramatically, with only 5% missing data between 1998 and 2015. Completeness of a data series is also a requirement for accurate EEMD results. Therefore, data at this site was analyzed beginning in January 1998.

Table 3.1. Names and locations of the 25 National Park Service Gaseous Pollutant Monitoring Program rural ozone monitoring sites

State	ABBR	National Park	Site	North Lat.	West Long.	Start Date	End Date	Elevation(m)
			Northwest					
AK	DENA-HQ	Denali	Headquarters	63.7258	148.9633	7/1/1987		661
WA	MORA-TW	Mount Rainier	Tahoma Woods	46.7583	122.1244	7/1/1991	10/1/2013	415
WA	NOCA-MM	North Cascades	Marblemount Ranger Stn.	48.5397	121.4472	2/1/1996	1/31/2008	109
WA	OLYM-VC	Olympic	Visitor Center	47.7372	123.1653	8/1/1985	2/28/2005	427
			West					
CA	DEVA-PV	Death Valley	Park Village	36.5092	116.8481	12/1/1993		125
CA	LAVO-ML	Lassen Volcanic	Manzanita Lake Fire Stn.	40.5403	121.5764	10/1/1987		1756
CA	PINN-ES	Pinnacles	SW of East Entrance Stn.	36.485	121.1556	4/1/1987		335
CA	SEKI-LK	Sequoia & Kings Canyon	Lower Kaweah	36.5658	118.7772	6/1/1984		1890
CA	YOSE-TD	Yosemite	Turtleback Dome	37.7133	119.7061	1/1/1992		3037
			Intermountain West					
TX	BIBE-KB	Big Bend	K-Bar Ranch Road	29.3022	103.1772	9/15/1990		1052
UT	CANY-IS	Canyonlands	Island in the Sky	38.4586	109.8211	7/1/1992		1809
MT	GLAC-WG	Glacier	West Glacier Horse Stbls	48.5103	113.9956	1/1/1992		976
NV	GRBA-MY	Great Basin	Maintenance Yard	39.0053	114.2158	8/24/1993		2060
AZ	GRCA-AS	Grand Canyon	The Abyss	36.0597	112.1822	1/1/1993		2073
CO	MEVE-RM	Mesa Verde	Resource Mngment Area	37.1983	108.4903	3/1/1993		2165
AZ	PEFO-SE	Petrified Forest	South Entrance	34.8225	109.8919	1/1/2002		1723
CO	ROMO-LP	Rocky Mountain	Long's Peak	40.2778	105.5453	1/5/1998		28
WY	YELL-WT	Yellowstone	Water Tank	44.5597	110.4006	6/1/1996		2400
UT	ZION-DW	Zion	Dalton's Wash	37.1983	113.1506	1/1/2004		1213
			East					
NC	GRSM-CM	Great Smoky Mountains	Cove Mountain	35.6967	83.6086	7/1/1988		1243
NC	GRSM-LR	Great Smoky Mountains	Look Rock	35.6331	83.9422	7/1/1988		793
KY	MACA-GO	Mammoth Cave	Great Onyx Meadow	37.2178	86.0736	12/1/1984	7/31/1997	219
KY	MACA-HM	Mammoth Cave	Houchin Meadow	37.1317	86.1481	7/1/1997		258
VA	SHEN-BM	Shenandoah	Big Meadows	38.5231	78.4347	5/1/1983		1072
MN	VOYA-SB	Voyageurs	Sullivan Bay	48.4128	92.8292	6/1/1996		429

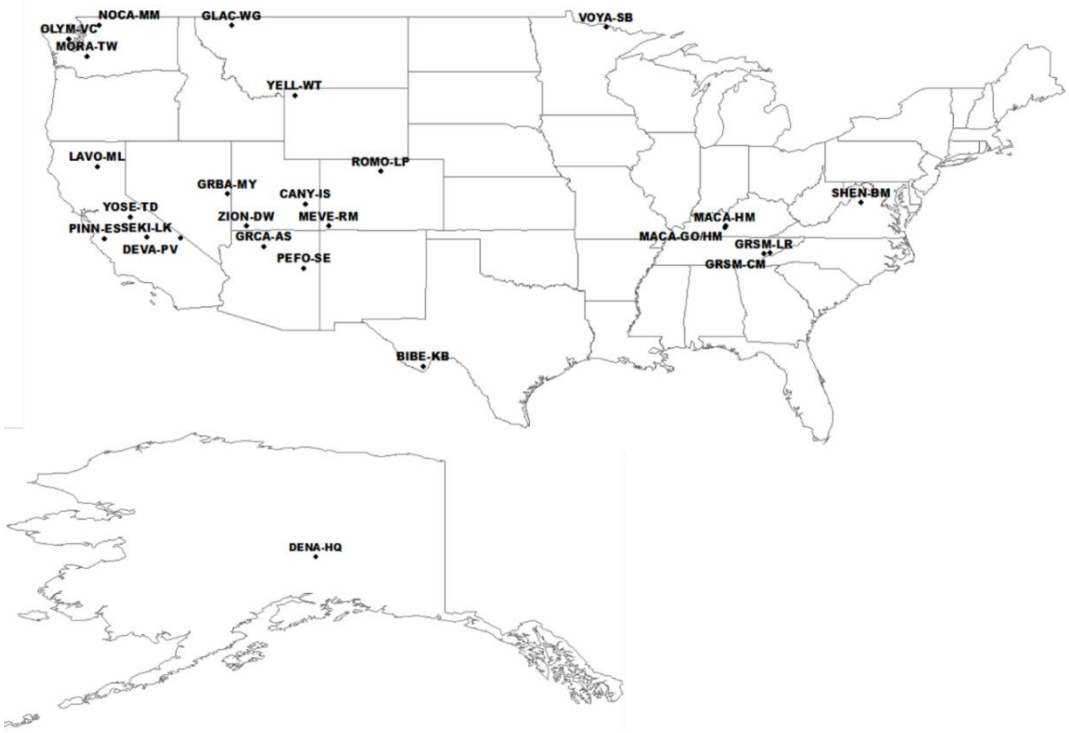

Figure 3.1 Locations of the 25 U.S. National Park Service sites used in this study.

For the assessment of variability in these data, the EEMD method [27] is used. The algorithm decomposes a time series into the temporal signals that make up its total variability. Specifically, a time series is broken down into *k* oscillatory components where components of higher frequency are extracted first. The oscillatory components or signals are referred to as Intrinsic Mode Functions (IMFs). The number of IMFs of a dataset was estimated to be $\log_2(N-1)$ [27,30], where N is the number of data points, which, in our case, was daily data averaged from hourly data. Component IMFs obey two properties: (i) the number of local maxima and minima differ at most by 1, and (ii) an IMF has a mean value of zero. The sifting process is repeated until the mean of the signal is sufficiently close to zero. After all of the signals are extracted from the time series, the residual (R_n) of the raw data results.

It is important to note that 12 components were extracted for all sites (determined by be $\log_2(N-1)$ but for shorter time series such as ZION-DW and NOCA-MM, the variance associated with components 11 and 12 is very small. This is because the time period associated with these components is longer than the length of these short data series therefore, components 11 and 12 do not complete a full oscillation at these sites. Therefore, data that is unable to be decomposed into components will end up in the residual and add to the trend. The percent variance that is contributed by lower frequency components such as 11 and 12 is under a percent. Therefore, these long-term components do not contribute significant uncertainty to the overall trend of shorter data sets.

The time derivative of R_n was calculated to determine the long-term trend in ozone at each site and the date on which the ozone trend changed, if at all. The trends resulting from the EEMD method are representative of the trends depicting ozone impacted by processes on multidecadal times scales. Some of the main factors that could have influenced ozone on

multidecadal timescales include the effect of regional ozone controls, land use and cover change, natural climate variability, and the 11-year solar cycle. It must be pointed out that this trend differs from the trends in baseline or background ozone that have been studied extensively in the current literature. The U.S. Environmental Protection Agency defines Policy Relevant Background (PRB) ozone as those concentrations that would occur in the U.S. in the absence of anthropogenic emissions in continental North America [31]. Background ozone needs to be quantified with the use of atmospheric models [31]. Baseline ozone is defined as ozone that has not been influenced by recent, locally emitted, or produced pollution [31]. Per the definition of background ozone and baseline ozone, both can be impacted by processes on time scales of days to decades, and certainly bear seasonal to interannual variations. In the literature, trends in background ozone reflect the trends in model simulated influence from outside of the study domain, which excludes changes in all sources, sinks, and processes inside the study domain, and is also affected by model uncertainties [7,14]. Trends in baseline ozone are measurement-based, but are mostly a singular trend, or lack thereof, for the entire study period. In comparison, the trend resulting from the EEMD method is one that does not include processes on time scales that are shorter than the variability on interdecadal timescales, and there could be more than one trend within the study period. To distinguish from the baseline or background trend in the literature, the trend that is identified in this study is referred to as the *multidecadal* trend.

To investigate the impact of atmospheric dynamics on ozone at one site, we used gridded datasets from the European Center for Medium Range Weather Forecasts (ECMWF) (http://www.ecmwf.int/) [32], including monthly 2.5° × 2.5° gridded reanalysis fields of zonal and meridional winds, as well as 500 hPa geopotential height for the study period 1987–2015. We also used the NOAA Hybrid Single Particle Lagrangian Integrated model (HYSPLIT),

dispersion version [33] to identify the origin of air masses of interest driven by NCEP/NCAR 2.5° × 2.5° meteorological data at the same site.

3.3 Results

The ozone data were decomposed into 12 oscillatory components using EEMD. For this study, we will focus on three of these components, including the 7th, 9th, and 10th component, and the residual, which were referred to as C7, C9, C10, and R_n, respectively. Our components of interest vary seasonally, interannually (by ENSO and PDO), and, as mentioned in Section 2, the residual R_n is the multidecadal variability. The components of interest at one site, ROMO-LP, are shown in Figure 3.2 as an example of EEMD results.

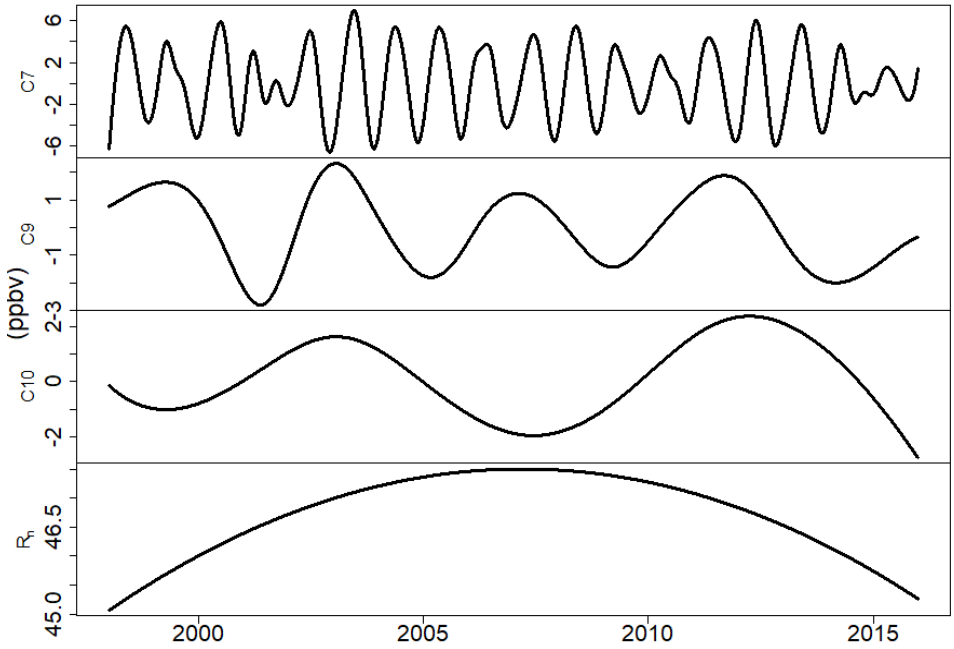

Figure 3.2: The four components (ppbv) of interest, C7, C9, C10, and R_n shown here for one site, Rocky Mountain National Park (ROMO-LP). Data capture at this site began in January 1987, but because of a data completeness requirement for EEMD, the start year for this site begins in 1998.

3.3.1 The multidecadal trend

The multidecadal trend in ozone, reported as the mean rate of change and one standard deviation of the mean and after the date of trend change for each site can be found in Table 3.2, and the spatial variability in trends can be found in Figure 3.3. It is worth noting that the trends at 20 out of the 25 sites changed from positive to negative at some point in time during the study period, and a clear divide in the date of the trend change was observed. Additionally, the trends at sites in closer proximity to regions of higher population changed before 2004, while those at sites in the West and Intermountain West changed during or after 2004. Therefore, the rates of positive and negative trends were identified with the date of trend change as occurring either before 31 December 2003 or after 1 January 2004. The monitoring at MACA-GO ended in 1997 and was replaced by MACA-HM, which is seven miles away, in the same year; therefore, trends in this region were considered to have changed from increasing to decreasing in the year 1997. Excluding MACA-GO, two sites exhibited constant increasing trends (BIBE-KB (TX) and GLAC-WG (MT)), and one with a constant decreasing trend (PINN-ES (CA)).

Table 3.2. Multidecadal ozone trend change (ppbv yr^{-1}) and date of trend changes. The trends in the 2nd and 4th column are the trends before and after the date of trend change, where the dates are indicated in the 3rd column. Sites in bold indicate that the trend changes occurred prior to 2004.

Site	Trend (ppbv yr^{-1})	Date of trend changes	Trends (ppbv yr^{-1})
		Northwest	
DENA-HQ	0.04 ± 0.02	1/8/2006	-0.02 ± 0.01
MORA-TW	**0.27 ± 0.15**	**7/20/2002**	**-0.32 ± 0.18**
NOCA-MM	**0.16 ± 0.10**	**7/21/2001**	**-0.20 ± 0.11**
OLYM-VC	**0.25 ± 0.15**	**1/13/1998**	**-0.08 ± 0.05**
		West	
DEVA-PV	0.23 ± 0.13	1/13/2007	-0.18 ± 0.10
LAVO-ML	0.23 ± 0.13	10/17/2007	-0.10 ± 0.06
PINN-ES	**-**	**-**	**-0.34 ± 0.10**
SEKI-LK	**0.08 ± 0.04**	**4/16/1997**	**-0.12 ± 0.07**
YOSE-TD	**0.07 ± 0.04**	**10/19/1998**	**-0.26 ± 0.15**
		Intermountain West	
BIBE-KB	0.11 ± 0.01	-	-
CANY-IS	**0.001 ± 0.001**	**2/10/2001**	**-0.08 ± 0.04**
GLAC-WG	0.18 ± 0.02	-	-
GRBA-MY	0.28 ± 0.16	9/16/2006	-0.20 ± 0.11
GRCA-AS	0.37 ± 0.21	9/28/2006	-0.25 ± 0.14
MEVE-RM	0.40 ± 0.23	8/15/2007	-0.24 ± 0.14
PEFO-SE	0.03 ± 0.02	3/21/2004	-0.23 ± 0.13
ROMO-LP	0.29 ± 0.18	3/6/2009	-0.25 ± 0.13
YELL-WT	0.19 ± 0.11	10/23/2006	-0.17 ± 0.10
ZION-DW	0.44 ± 0.26	12/16/2008	-0.63 ± 0.37
		East	
GRSM-CM	**0.07 ± 0.04**	**1/18/1995**	**-0.35 ± 0.20**
GRSM-LR	**0.35 ± 0.20**	**7/18/2003**	**-0.35 ± 0.20**
MACA-GO*	0.09 ± 0.01	-	-
MACA-HM*	**-**	**-**	**-0.60 ± 0.01**
SHEN-BM	**0.37 ± 0.21**	**10/27/2002**	**-0.27 ± 0.16**
VOYA-SB	**0.26 ± 0.15**	**10/21/2003**	**-0.44 ± 0.25**

*The monitoring at MACA-GO ended in 1997 succeeded by MACA-HM, 7 miles away, in the same year, and therefore trends in this region were considered to have changed from increasing to decreasing in the year 1997.

Of the sites in the western half of the U.S., positive trends were the lowest mostly in Central California and Texas, ranging from 0.07 to 0.11 ppbv $year^{-1}$, while stronger positive trends of 0.37–0.44 ppbv $year^{-1}$ were found largely in the Intermountain West at GRCA-AS, MEVE-RM, and ZION-DW (Figure 3.3a). Trends in the West changed from positive to negative over a broad range of time, between 1997 and 2008 (Table 3.2). Within that time period, three

sites changed from positive to negative prior to 2004 and nine sites after 2004. Ozone levels have been trending downward at 17 of the 19 western sites at rates that range between −0.02 to −0.63 ppbv year^{-1}, since their respective dates of trend change (Table 3.2). The strongest negative trends in the West were found at ZION-DW at −0.63 ppbv year^{-1}, followed by PINN-ES, at −0.34 ppbv year^{-1}. Note that PINN-ES exhibited a constant decreasing trend averaging −0.34 ppbv year^{-1} throughout its monitoring period (1987–present). Trends at SEKI-LK and YOSE-TD, located in the west, changed from positive to negative in 1997 and 1998, respectively, marking these two sites the second and third to change their trend status from positive to negative, while GRSM-CM, located in the east, changed trends status in 1995, marking this as the first site, to change its trend status from positive to negative. CANY-IS, which is located in southeastern Utah, is the fourth site to shift to negative prior to 2004 and is the only site in the Intermountain West to change trend status from positive to negative prior to 2004. Of the nine sites with a change from positive to negative after 2004, all but CANY-IS are located in the Intermountain West, excluding LAVO-ML, which is located in northern California.

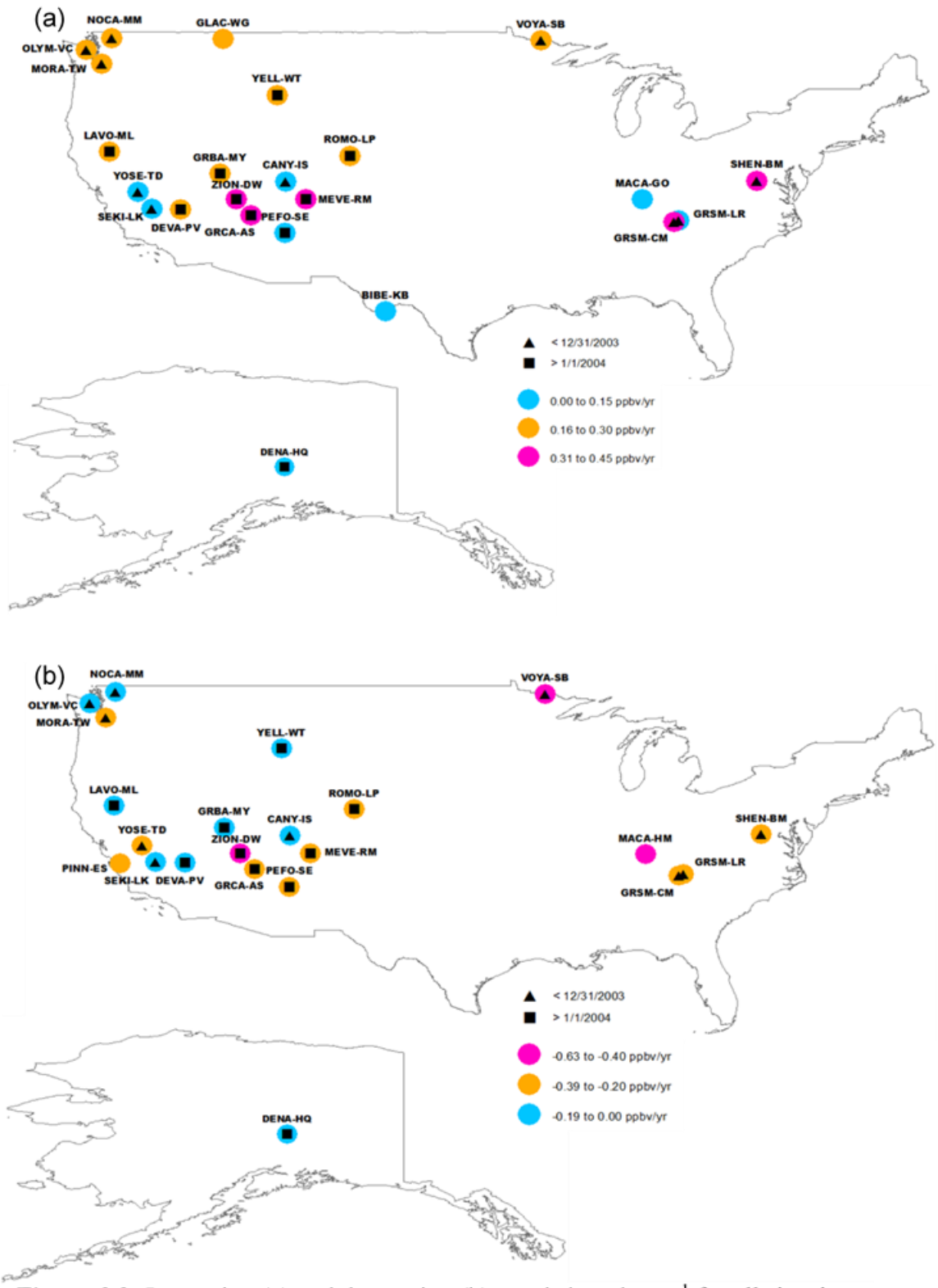

Figure 3.3: Increasing (a) and decreasing (b) trends in ppbv yr^{-1} for all sites in the study. The date of trend changes from positive to negative are symbolized for each site. Sites that changed prior to 12/31/2003 are symbolized by triangles and sites that changed after 1/1/2004 are symbolized by squares.

At GLAC-WG (MT) and BIBE-KB (TX), ozone trends have been increasing at 0.18 and 0.11 ppbv $year^{-1}$ since the start of monitoring in 1992 and 1990, respectively. Both of these sites have exhibited a leveling of ozone trends beginning in 2014, but neither site has shown a reversal of trends. DENA-HQ had a weakly positive trend of 0.04 ppbv $year^{-1}$ between 1987 and 2006, at which point the trend shifted downward at a rate of −0.02 ppbv $year^{-1}$. In the East, trends at all of the sites changed from positive to negative prior to 2004. Rates of positive trends ranged from 0.07 ppbv $year^{-1}$ at GRSM-CM to 0.35 ppbv $year^{-1}$ at GRSM-LR. GRSM-CM had a trend shift from positive to negative, the earliest of all sites, but also had the weakest positive trend. Since 2004, ozone has been trending downward at all five of the eastern sites (MACA-GO is no longer monitoring). Overall, surface ozone levels are decreasing at 22 of the 25 NPS sites across the U.S.

3.3.2 The Seasonal Cycle

The ozone seasonal cycle (C7), considered to be changing with the seasons but having one peak and one minimum per year, has varied in timing and amplitude at several sites. The most distinctive feature of the seasonal cycle is the spring/summer maximum and fall/winter minimum at all sites, which is characteristic of the Northern Hemisphere [34,21,22]. DENA-HQ has a very different seasonal cycle from the other sites in the study domain, with maxima in late March and minima in late August. Of all the components, the seasonal cycle contributed the greatest, 31.8% on average, of the total variance. Therefore, the seasonal cycle is the most important characteristic of the data controlling variation in ozone.

3.3.2.1 Change in Amplitude of Seasonal Cycles

The annual amplitude is the difference in ppbv between the annual ozone maximum and minimum. To determine significant changes in annual amplitude, linear regression was

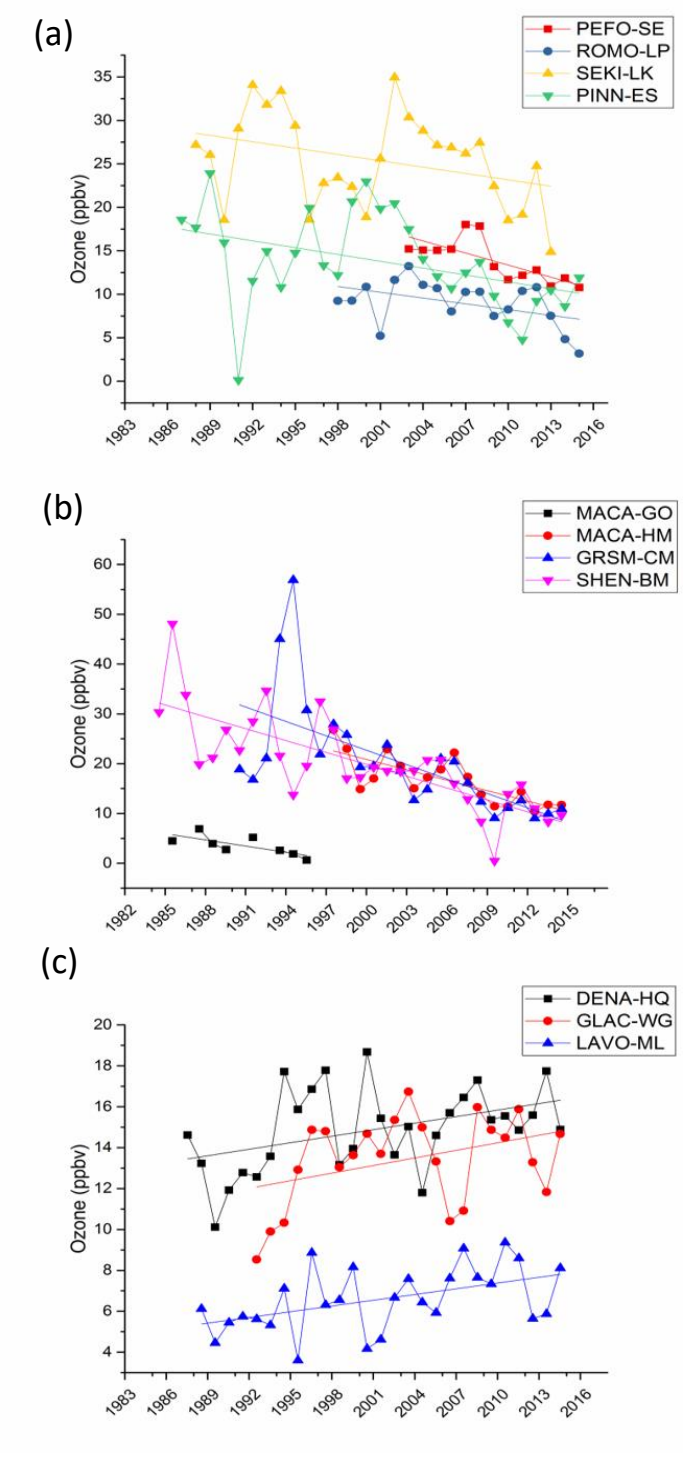

Figure 3.4: Sites with a significant negative change in annual amplitude for western (a) and eastern sites (b) and a significant positive change in annual amplitude (c).

performed. The magnitude of annual amplitude decreased significantly ($p < 0.10$) by 5 to 20 ppbv at four sites in the West and four sites in the East during their respective monitoring periods (Figure 3.4a,b; Table 3.1). Amplitude decreases in the West ranged between 5–7 ppbv for all four sites (Figure 3.4a), while the sites in the East have decreased by 5 ppbv at MACA-GO, 10 ppbv at MACA-HM, and 20 ppbv at GRSM-CM and SHEN-BM during their respective monitoring periods (Figure 3.4b). Stronger amplitude decreases were observed in the East than in the West, and proportionately more sites experienced decreases in the East than the West. Three sites had significant increases in annual amplitude, none of which were located in the East (Figure 3.4c). Specifically, LAVO-ML, which is located in northern

California, had an increase of 3 ppbv between 1987 and 2015. DENA-HQ had an increase of 4 ppbv over the same time-period. GLAC-WG had an overall increase of 3 ppbv between 1992 and 2015. In comparison, sites with increases in annual amplitude were not as significant in magnitude as sites with decreases in annual amplitude.

3.3.2.2 Change in Timing of Seasonal Cycles

A shift to earlier in the year was observed in the annual maximums and minimums at 12 of the 25 sites. Sites with a significant shift are indicated in Figure 3.5. Figures 3.5a and b depict the nine sites that had a significant shift in peak date with 5 in the West, including the one site in Alaska (DENA-HQ) (Figure 3.5a), while Figure 3.5b shows four sites in the East. The sites with significant peak shifts in the West had shifted 10 to 60 days earlier during their respective monitoring periods (Figure 3.5a), while in the East, sites have moved 35 to 60 days earlier (Figure 3.5b). A closer examination revealed that the annual peaks at eight of the nine sites occurred in June and July prior to 2000, but afterward gradually shifted to late April/early May (Figure 3.5a,b). The annual maxima at DENA-HQ in Alaska shifted earlier by 10 days from early April in 1987 to late March beginning around 2003 (Figure 3.5b). Eight sites had an earlier occurring annual minimum, while four of these sites also had a shifting annual maximum (Figure 3.5c,d). Five of the eight sites with shifting annual minima were in the West, while the other three reside in the East. The annual minimum shift was more significant in the three eastern sites (28–34 days) than the five western sites (14–21 days).

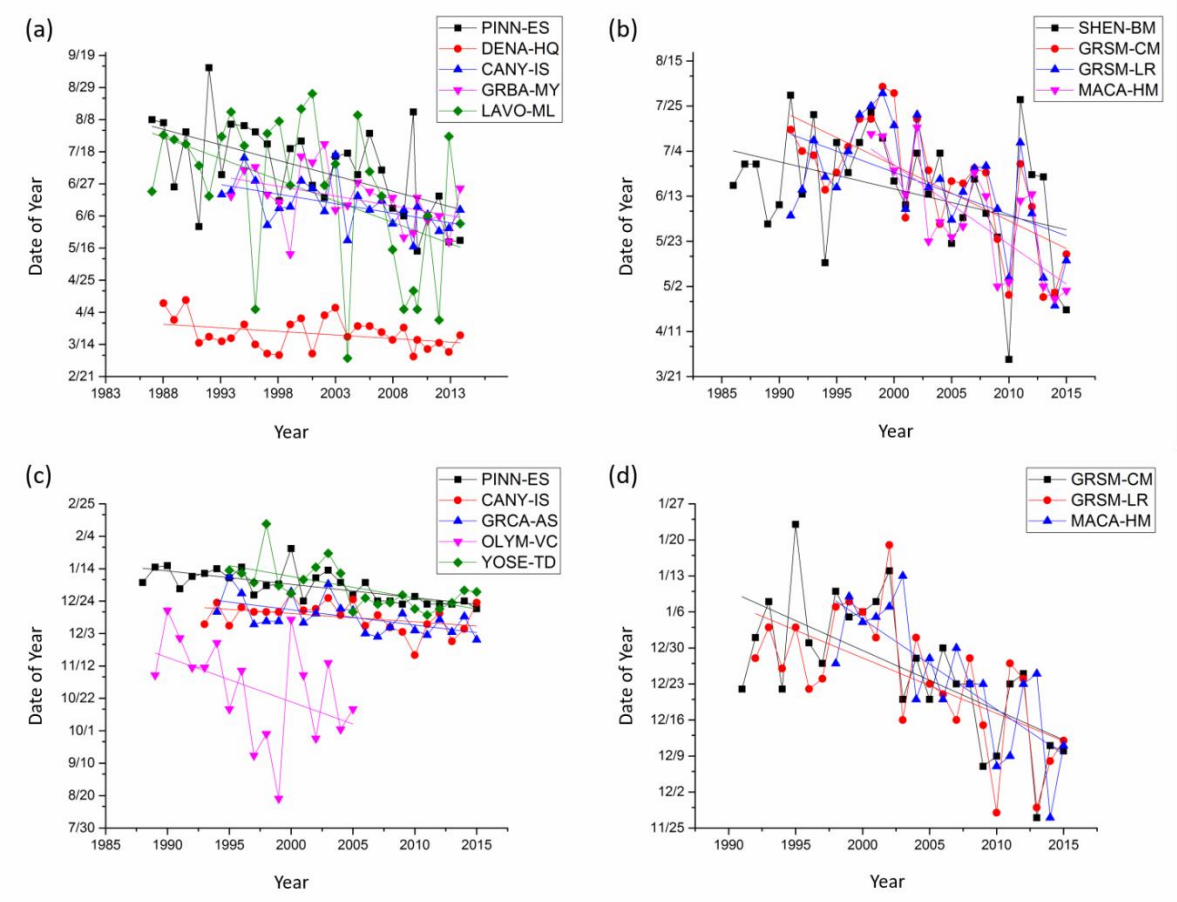

Figure 3.5: Significant shifts in the date of annual ozone peak values for the western (a) and eastern (b) sites. Significant shifts in the date of annual ozone minimum values for western (c) and eastern sites (d).

Proportionately more sites in the East had a shift in the seasonal cycle than in the West for both the annual maximum and minimum. Of the nine sites with significant changes in the annual amplitude, six had significant ($p < 0.10$) changes in the date of annual maximums and minimums (SHEN-BM, GRSM-CM, MACA-HM, PINN-ES, DENA-HQ, CANY-IS, LAVO-ML), while three had insignificant ($p > 0.10$) shifts to an earlier date (GRSM-LR, MACA-GO, GRBA-MY). Conversely, only three sites with significant changes in amplitude had significant shifts in the minimum date (PINN-ES, GRSM-CM, and MACA-HM).

3.3.3 Variability by Large-Scale Climate Circulation Linked to Components C9 and C10

Surface temperature data have been widely analyzed and its time scales have been identified in the literature [10,35,36]. Zhang et al. [36] examined the correlation of the Precipitation Condition Index, Vegetation Condition Index, and decomposed precipitation and temperature data with the Niño 3.4 SST index. They identified the lag and correlation coefficient between this climate mode and the components representing ENSO to determine if ENSO was the main driver of variability [36]. However, the correlation and lag response of a variable that is associated with PDO is not as clear. Therefore, given the robustness of EEMD and the suggested linkage between ENSO/PDO and surface temperature [35,37], surface temperature data at each site (obtained from the same source as the ozone data used in this study) were decomposed by EEMD and were used as a proxy to determine if there was a similar linkage between ENSO/PDO and surface ozone. The EEMD time scales for components 9 and 10 for temperature oscillate every 3–7 years and 9–12 years, respectively, which match with the variability identified for ENSO and PDO [38,39].

Further, correlation coefficients between component 9 (C9) and component 10 (C10) for temperature and ozone were calculated. Given that both of the components are distributed nonparametrically, correlation coefficients were determined using the Spearman Rank Order Correlation test. Resulting correlation coefficients for each site are shown in Figure 3.6. Values of significance for correlation coefficients between C9 for temperature and ozone were all within the 95% confidence limit, except for DENA-HQ ($p = 0.24$) and MACA-GO ($p = 0.21$). Values of significance for correlation coefficients between the two C10 signals were all within the 95% confidence limit. C9 correlation coefficients (Figure 3.6a) were strongly correlated ($r > 0.5$ or $r < -0.50$) at 2 of 25 sites and were weakly correlated ($0.25 < r < 0.5$) at 10 of 25 sites. Signal C9 of

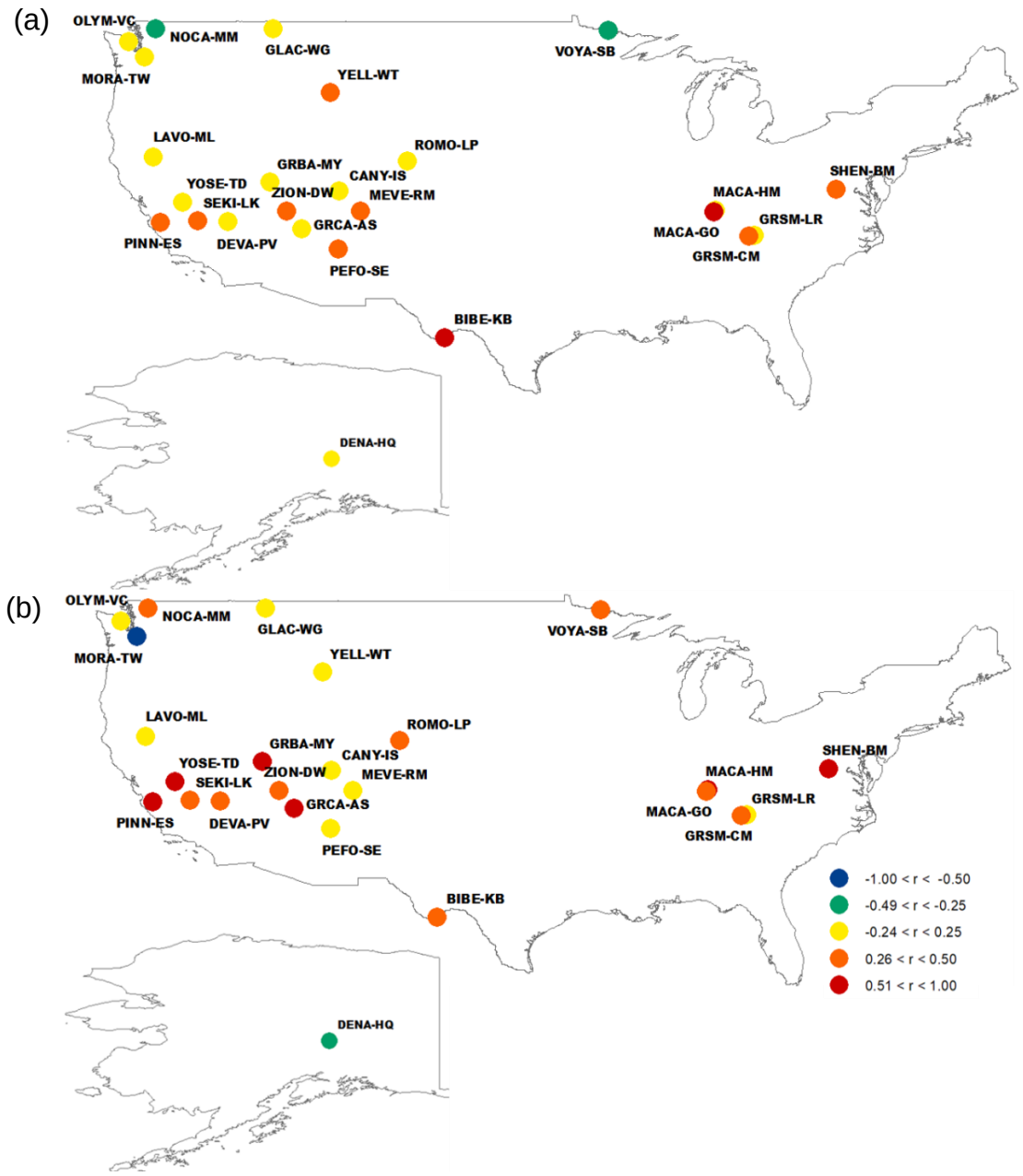

Figure 3.6: Spearman rank correlation coefficients between the C9 components for ozone and temperature (a), and the C10 components for ozone and temperature (b).

ozone oscillates on a similar timescale to this component in temperature therefore, it is suggested to represent ENSO. Its significant correlation with that of ozone thus indicated the contribution of ENSO to surface ozone. Signal C10 in temperature and ozone were strongly correlated ($r >$ 0.50 or $r < -0.50$) at 8 of 25 sites and were weakly correlated ($0.25 < r < 0.50$ or $-0.25 < r <$

−0.50) at 9 of 25 sites (Figure 3.6b). Signal C10 for ozone oscillates about every 8–12 years, which is a similar time scale to temperature, and was thus suggested to represent PDO. Its correlation with C10 in ozone hence alludes to the same process driving ozone.

Individually, components C9 and C10, or variability by ENSO and PDO, contribute about 1–2% to the variance in ozone concentrations. However, both of the components have a modulating effect on the seasonal cycle as well as subsequent higher frequency components. The modulation effect of lower frequency signals on higher frequency signals can be illustrated using the seasonal cycle of Rocky Mountain National Park (ROMO-LP). In Figure 3.7, signals of the seasonal cycle (C7), ENSO (C9), and PDO (C10) for Rocky Mountain National Park (ROMO-LP) are superimposed. Black arrows indicate that ENSO and PDO are out-of-phase, while gray

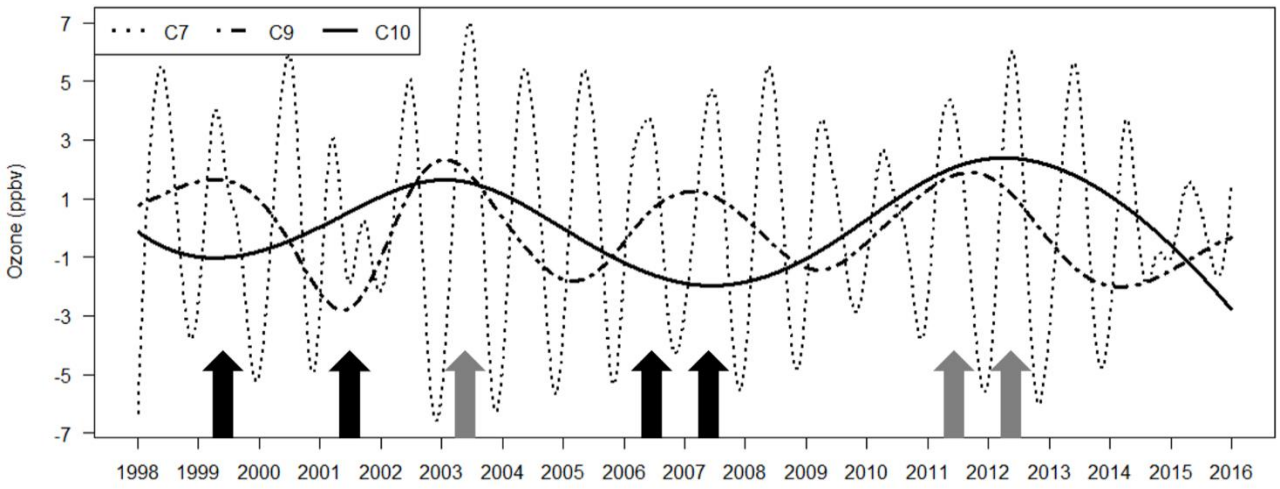

Figure 3.7: The various effects of C9 and C10 on C7, the seasonal component, depending on the cycle phase. Black arrows indicate that C9 and C10 are out-of-phase; grey arrows indicate that the components are in-phase.

arrows indicate that the components are in-phase. For example, in spring 2003, 2011, and 2012 the seasonal cycle was enhanced by 3–4 ppbv from the previous year, while ENSO and PDO were in phase. Therefore, when ENSO and PDO act in concert and the regimes in these climate modes have reached a peak, maximums in the seasonal cycle were enhanced. Modulation, or the

enhancement of the seasonal cycle, by lower frequency components occurs at all sites in the study domain.

3.4 Discussion

3.4.1 Impacts of Domestic Emissions Reductions on Rural Ozone Trends

Declining trends were found to be −0.27 to −0.6 ppbv yr^{-1} in the East and −0.02 to −0.63 ppbv yr^{-1} in the West/Intermountain West (Figure 3.3b). The most significant trend decreases in the West/ Intermountain West were seen at ZION-DW with decreases at a rate of -0.63 ppbv yr^{-1}. The second most significant decreases in this region were seen at PINN-ES, where decreasing trends (Figure 3.3b) were observed throughout the monitoring period (Figure 3.1). This site has some of the earliest ozone measurements in the study domain, beginning in 1987, and is currently still monitoring. The eastern U.S. has the earliest shift in trend status from positive to negative (with sites in central California and the Northwestern U.S. following suit thereafter (Table 3.2). The first sites in the west to change from positive to negative trends were SEKI-LK (16 April 1997) and YOSE-TD (19 November 1998), which are the closest in proximity to PINN-ES (Table 3.2; Figure 3.3). It should be noted that, of the sites with the earliest shift from positive to negative (1995–2003), all of them are located near urban regions, which include central California, Northwestern Washington, and the Eastern U.S., which have experienced more significant decreases in ozone trends relative to rural areas [9]. This trend was found by Cooper et al. [9] but it should be pointed out that their work did not include sites in the Northwestern U.S. Three sites in this work MORA-TW, NOCA-MM, and OLYM-VC are located in the Northwest and are in close proximity to the Seattle metropolitan area. The timing of the ozone reductions within the greater Seattle metropolitan area coincides with the findings of Simon et al. [3], which showed that both NO_x and VOC emissions decreased by 39.6% and

14%, respectively, in the Northwestern U.S. between 2000 and 2011. The decrease in these precursor emissions likely facilitated the decrease in ozone for MORA-TW, NOCA-MM, OLYM-VC

Cooper et al. [9] identified the Denver Metropolitan area as a region that did not have significant reductions in ozone precursor emissions, while they attributed Los Angeles Basin ozone decreases to VOC emission reductions, based on nation-wide emission inventories within the 1980–1995 time period. The U.S. EPA's State Tier 1 database reported Colorado's estimated 2000 NO_x emissions were reduced by 1762 tons when compared against 1990 levels, decreasing from 33,381 tons to 31,619 tons, for a 5.3% reduction [40]. California's estimated NO_x emissions between the same period were reduced by 16.0%, decreasing from 171,382 tons to 143,936 tons, for a reduction of 27,446 tons [40]. This difference in emission reduction could explain why decreasing trends in ozone were not observed until 2009 at ROMO-LP, which is located downwind of the Denver Metropolitan region (Table 3.2) [40]. In contrast to Colorado, the Los Angeles Basin, ozone levels decreased by 50 ppbv between 1979 and 1997 (followed by no decreases over 1997–2008), which is potentially the cause of the earlier start of decreasing trends in ozone at two sites downwind of Los Angeles (YOSE-TD and SEKI-LK). PINN-ES has exhibited a decreasing trend in ozone since its inception as an ozone monitoring site, but it is in relatively close proximity to the coast when compared to the other central California sites where it is influenced by marine air; therefore, it is less likely to be affected by the Los Angeles Basin, like the other central California sites. In the eastern states of Virginia and Kentucky and the western states of Washington and California, where all of the sites with the earliest of trend reversals are located (prior to 2004), the State Tier 1 NO_x emission reductions between 1990 and 2000 were −12.0% in VA, −10.5% in KY, −14.3% in WA, and −16.0% in CA [40]. The earliest

emission reduction implementation in the Intermountain West occurred in the Denver Metropolitan area of Colorado in 1997. However, many states in the Intermountain West have seen a significant shift in source sectors, in addition to increases in frequency and magnitude of wildfires [41–44], all of which may be influencing the increasing ozone trends that were observed at BIBE-KB and GLAC-WG.

3.4.2. Variability in the Seasonal Cycle of U.S. Surface Ozone

Parrish et al. [18] suggested several hypotheses to explain the shift in the seasonal cycle which include changes in precursor emissions and ozone photochemistry, variability in transport pathways, and climate factors. Emission reductions have likely impacted the trends in ozone at sites nearest large urban areas, which could have also affected the annual amplitude and the shift in seasonal cycles. Rising springtime ozone of ~0.6 ppbv $year^{-1}$ in the western U.S. from 1984 to 2008 was identified by Cooper et al. [24,26], and was thought to result from the changing distribution of ozone precursors; this subsequently caused the shift in seasonal cycles and decreased annual amplitude [26]. Specifically, decreased NO_x emissions could have decreased annual ozone peaks, but it also reduced ozone removal via NO titration [25], the latter of which has led to increased wintertime and early springtime ozone levels [4,9,18,45]. Hence, increased springtime ozone and decreased summertime ozone may be a key driver of the shift in the ozone annual peak to earlier in the year [26].

There was greater regional continuity in the East than the West, with four out of six sites showing significant decreases in the magnitude of annual amplitude (Figure 3.4b), four out of six sites with a significant shift in annual maximum (Figure 3.5b), and three out of six sites with a significant shift in annual minimum (Figure 3.5d). In comparison, 5 out of 19 west coastal sites have had changes in the magnitude of annual peaks and minimums. Of the sites in the West,

three out of four sites had significant decreases in annual amplitude. Three out of five, and four out of five sites for annual maximum and minimum, respectively, were located in the regions with the earliest shift in trends from positive to negative (Figure 3.5a,c). Parrish et al. [18] suggested that the shift in the seasonal cycle may be a phenomenon occurring across northern mid-latitudes. Our study suggests that this shift did not seem to occur uniformly at all mid-latitudinal locations, as overall across the U.S. 9/25 (8/25), NPS sites have had a change in timing of annual maximums (minimums), and 11/25 have had a change in annual amplitude.

3.4.3. Effects of Large-Scale Climate Circulation on Seasonal cycles of U.S. Surface Ozone

Studies have suggested that various modes of climate variability and related dynamical mechanisms are responsible for the changes in free tropospheric and surface ozone [5,7,43–46]. Lin et al. [6,8,48] investigated the impact of large-scale climate perturbations on U.S. surface ozone trends using a global chemistry climate model, and their results show that they have a clear impact on the seasonal variability in ozone. For instance, the positive PDO over 1977–1998 was accompanied by stronger and more prolonged El Niño events, followed by a negative PDO between 1999 and 2015 with stronger and more prolonged La Niña events. [8]. This has implications for the transport of East Asian pollution and subsequently the seasonal cycle of U.S. surface ozone.

The dynamics of PDO and ENSO could explain the modulatory effect of ENSO and PDO on the seasonal cycle of ozone at the majority of the NPS sites, as shown in Section 3.3. In the positive phase of ENSO and PDO, zonal winds in winter are heightened [8,38,49]. This manifests as an increase in transpacific transport of Asian pollution to the southwestern U.S. via a strengthened subtropical jet stream in late winter and early spring [10,50], likely leading to springtime ozone and perhaps higher annual maximum ozone there. During La Niña and

negative PDO periods, the northward shifting subtropical jet stream directs East Asian pollution to the Pacific Northwest [6,51], likely increasing the surface ozone levels in Alaska and the northwestern U.S., whereas in other parts of the U.S. surface ozone was lowered. The long term increasing trend in surface ozone in Alaska will be discussed further in Section 4.4. In addition to variability in transport, El Niño episodes bring warm and dry conditions to the central and southern part of the country, ripe conditions for ozone formation [38], whereas La Niña episodes bring increased storms and cloudiness as well as cooler temperatures; therefore, ozone formation is not as strong during La Niña periods [38]. This also seems consistent with the modulatory effect of ENSO/PDO on the seasonal cycle.

3.4.4 Increasing Annual 4th-Highest DM8HA and Annual Amplitude of Ozone at DENA-HQ over 1987–2015

Denali National Park (DENA-HQ) (63.7258° N, 148.9633° W) is the only location where an increase in annual amplitude was found throughout the monitoring period. The annual maximum DM8HA value increased by 2 ppbv between 1987 and 2015 (Figure 3.4c), while the annual minimum value decreased by 2 ppbv (Figure 3.5a). In addition to this, there has been a statistically significant increase in the annual 4th-highest DM8HA. The annual 4th-highest DM8HA is found to be increasing at a rate of 0.33 ppbv year^{-1} ($R^2 = 0.29$, $p < 0.05$) (a total increase of ~9 ppbv) (Figure 3.8). The annual 4th-highest DM8HA does not occur during DENA-HQ's peak ozone season of late March to early April, but rather late April to May. This is likely due to the influence of higher solar irradiance coupled with transpacific transport [52]. It is important to note that the overall multidecadal trend at this site has not changed. However, the increasing trend in the annual 4th-highest DM8HA coupled with the increase in annual peak ozone values could signal the beginning of a multidecadal ozone trend increase at DENA-HQ in

the future. As aforementioned, the persistence of the negative PDO since 1998–1999, concurrent with more La Niña events, has resulted in a shift in transport of East Asian pollution to higher latitudes (45°–50°), which has subsequently increased the number of polluted air masses that are arriving to this region. To demonstrate the influence of polluted air masses that are transported from East Asia to DENA-HQ, back trajectories were conducted for the seven days before and after the date of the annual 4th highest DM8HA value occurrence at 22:00 UTC (14:00 Alaskan time), the average 8-hour rolling average start time for two time periods, 1987–1998 and 1999–

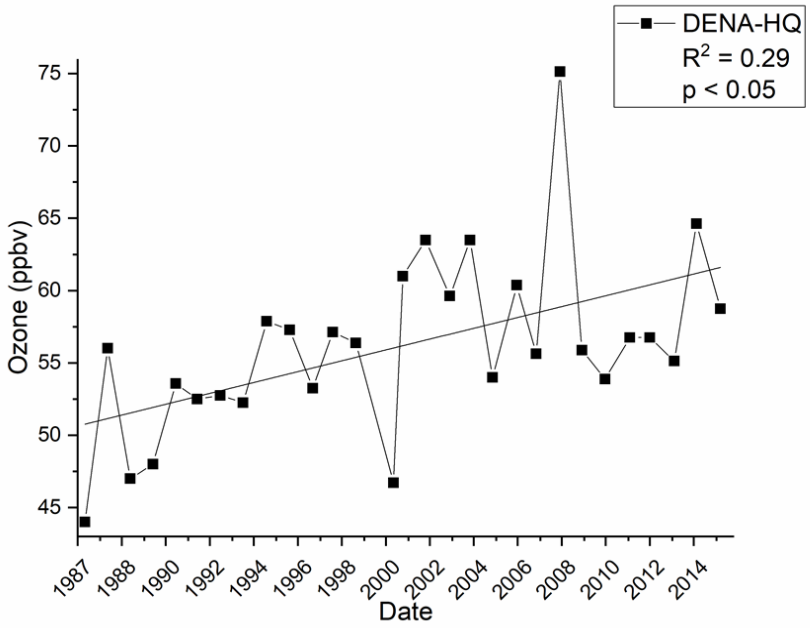

Figure 3.8: The annual 4th highest DM8HA at Denali National Park in Alaska (DENA-HQ) and a best fit linear regression line showing a coefficient of determination of 0.29.

2015. Of the 29 DM8HA values for the DENA-HQ record, 27 of them occurred in the months of April or May. Seven day back trajectories were calculated from DENA-HQ during these months, following the works of Jaffe et al. [53], Berntsen et al. [54], Yienger et al. [55,56], and Holzer et al. [57], which found that the average transport time in the spring between North America and

Asia was ~7 days. These trajectories were plotted and the area around the arrival point (DENA-HQ) was divided into eight sectors of 45° (Figure 3.9).

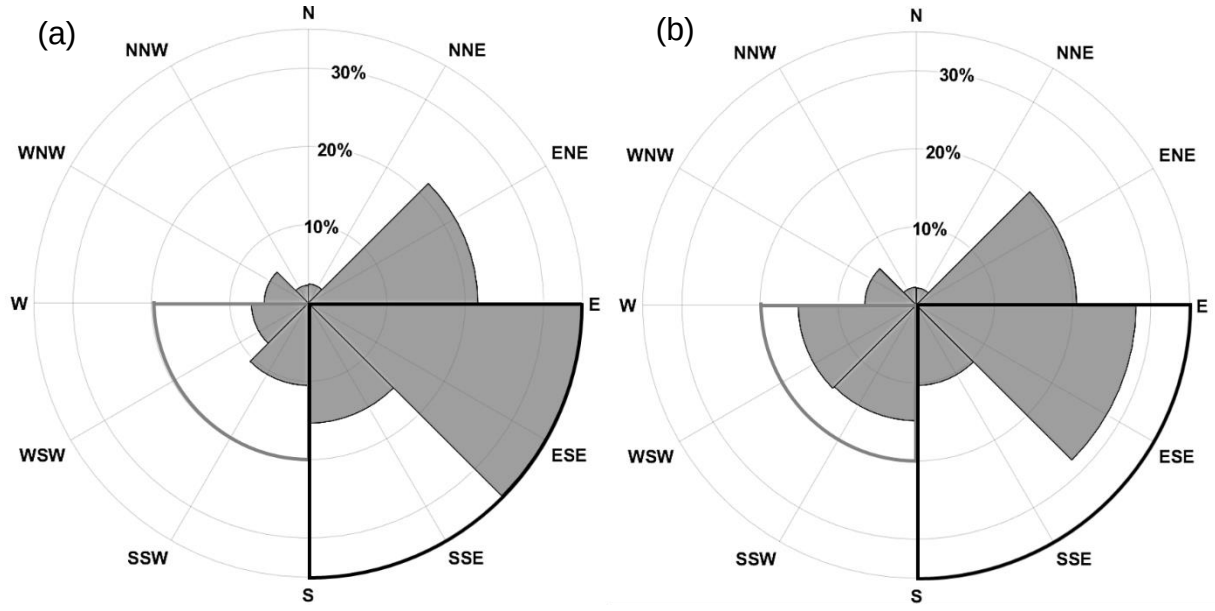

Figure 3.9: The percent of trajectories that fell in 8 radial sections around DENA-HQ. Rolling 7-day back trajectories were calculated using the HYSPLIT model. Trajectories were calculated seven days before and after the date of the annual 4th-highest DM8HA at DENA-HQ for the periods 1985 - 1998 (a) and 1999 - 2012 (b). The grey boxes indicate the area where an increase in trajectories were seen from period one (a) to period two (b) and the black box indicates where a decrease in trajectories were seen from period one (a) to period two (b).

Over 1987–1998, 72% of trajectories were from the area East-North-East to South (ENE–S) of DENA-HQ (Figure 3.9), which suggests that the majority of air masses that are arriving at the site originated from the marine boundary layer and western Canada. Over 1999–2015, 13% more trajectories came from West to South (W–S) of DENA-HQ, while 12% less from the east-south directions when compared to the 1987–1998 period. This means that during the time period from 1999 to 2015, air mass transport was more frequent from the North Pacific, with an increased potential of transporting East Asian pollution to DENA-HQ, and less frequently from above the Arctic Circle over land and near coastal regions of Canada, where the air is mostly pristine.

To determine the key factors driving the variability in the direction of backward trajectories between the two periods (1987–1998 and 1999–2015) for the months of April and May, monthly mean geopotential height fields with wind speeds at 500 hPa for 1987–2015, 1987–1998 (period one), and 1998–2015 (period two) were examined for April and May during each period (Figure 3.10). Anomalously low geopotential heights occurred to the west of Alaska for period one (Figure 3.10b); during period two, anomalously high geopotential heights occurred in the same area (Figure 3.10c). These findings are in agreement with Bond and Harrison's [58] study on the variability and relationship between ENSO and the Arctic Oscillation on the climate of Alaska, but for the winter months of November through February. The increased number of El Niño events that occurred during the positive PDO phase over 1987–1998 resulted in a low-pressure system to the southwest of Alaska during April and May, the months when transport over the Pacific is the greatest [57], allowing for air masses to preferentially move from the U.S. West Coast and the marine regions south of Alaska. During the second period 1999–2015 in the months of April and May, a high-pressure system resulted in increased westerly flow across the North Pacific to DENA-HQ and a decrease in the air masses from the marine regions south of Alaska. Air masses originating from this region for the week before and after a peak ozone event at DENA-HQ are presumably more polluted. It is likely that there was pollution outflow during these times from East Asia, causing the increase in ozone at this site. Therefore, the changing circulation regimes enhanced the transport of western polluted air masses to Alaska during period two, ultimately leading to the increasing trends in the annual 4^{th} highest DM8HA values and the magnitude of the annual amplitude after 1999 at DENA-HQ.

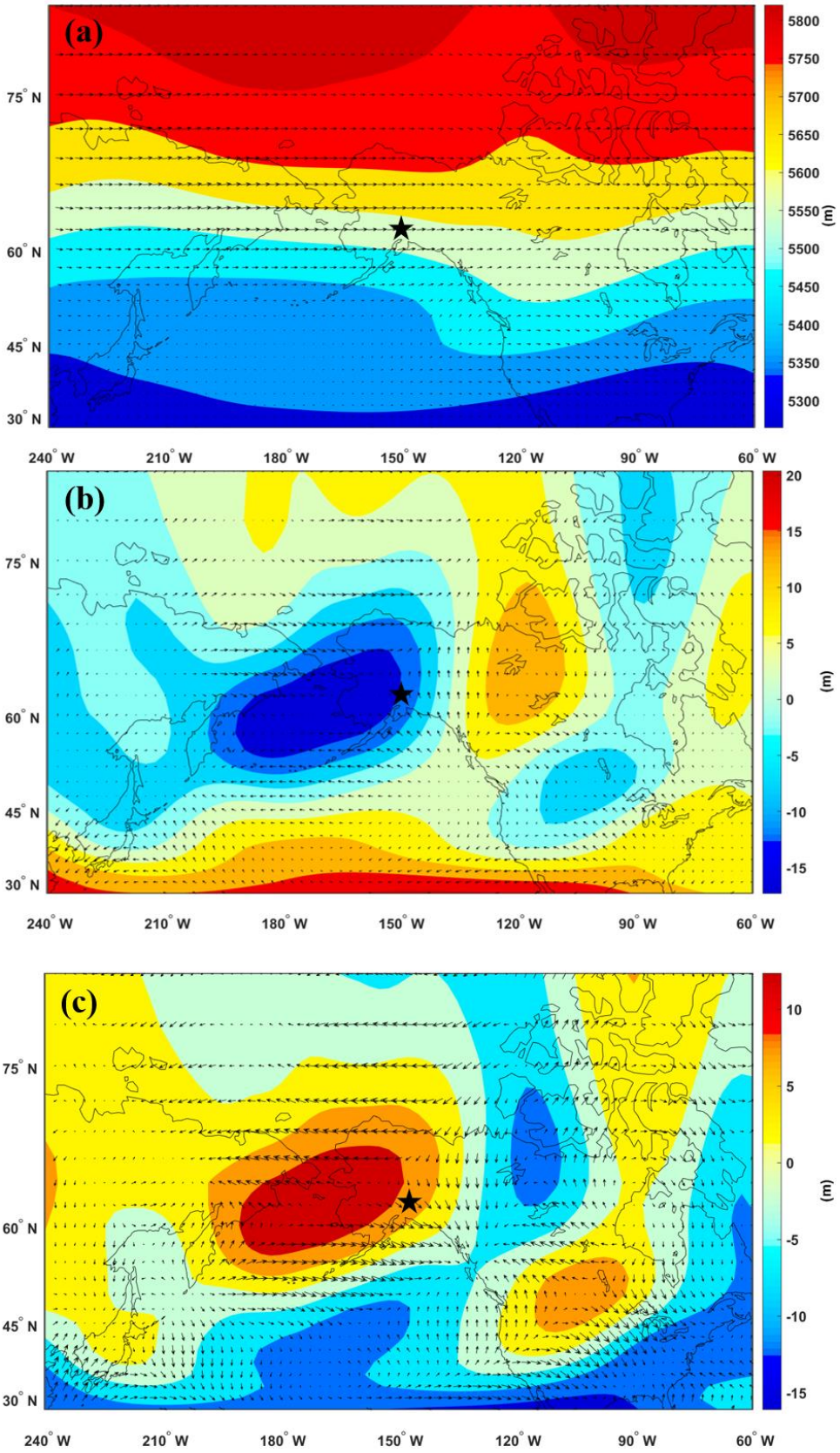

Figure 3.10: (**a**) Mean geopotential height in meters (colored contours) and mean wind speed in m/s (wind vectors) at 500 hPa for April–May of 1987–2015. Anomalous geopotential height and wind speed were calculated and plotted for the period April–May of 1987–1998 (**b**) and 1999–2015 (**c**).

3.5 Summary

In this study, 25 U.S. NPS datasets were analyzed for spatial and temporal variability in long-term ozone using EEMD. This method has allowed for an analysis of the spatial and temporal variability of long-term ozone data on four time-scales, which include seasonal, interannual, interdecadal, and multidecadal. Peak values in the ozone seasonal component have shifted to earlier in the year at nine sites by 10–60 days, while minimum values have shifted to earlier in the year at eight sites by 14–34 days. There has been a decrease in annual maximum values and an increase in annual minimum values at eight sites by 5–20 ppbv $year^{-1}$. The changes that were seen in the seasonal cycle were likely the result of decreasing NO_x concentrations that would result in a change in the distribution of ozone throughout the year, leading to an increase in minimum ozone values and a decrease in maximum ozone values. Interannual and interdecadal cycles resulting from ENSO and PDO have a constant effect on higher frequency components. This effect was examined using the seasonal component where we found the greatest enhancement in ozone concentrations of 3–4 ppbv in the annual maximum value when ENSO and PDO were both positive and in-phase. Multidecadal trends were identified to change from increasing to decreasing at 20 of the 25 sites. Increasing trends were found to be between 0.001 ppbv and 0.4 ppbv $year^{-1}$, while decreasing trends were found to be between −0.02 to −0.63 ppbv $year^{-1}$. The multidecadal trend shifted from positive to negative prior to 2004 at sites in the Eastern U.S., Southern California, and the Pacific Northwest. In the Intermountain West, trends shifted from positive to negative most predominately after 2004. Decades of increasing annual amplitude, annual 4^{th} highest DM8HA, as well as a shift in date for both of these variables at Denali National Park in Alaska (DENA-HQ) may have resulted from a change in transport pathways related to the PDO. These changes likely stemmed from an

increase in the strength and longevity of La Niña events over 1999–2015, and a negative PDO period, which increased the transport of heavily polluted air masses from East Asia by 13% from the previous PDO period of 1987–1998.

The findings from this study can be used to aid in future ozone mitigation strategies and policies in the United States. For example, the US EPA requires large energy plants to keep NO_x emission below a certain budget during the ozone season of May to September [59]. In this study, we found that peak ozone concentrations were occurring as early as March at some sites. Therefore, the period of decreased NO_x emissions should be pushed earlier in areas that peak ozone is occurring out of the ozone season. The modulatory effects of large circulation processes on higher frequency components can be useful in predicting high ozone events in the U.S. A more extensive analysis incorporating other components of the ozone data sets is warranted to better understand and assess the impact of major climate modes on U.S. ozone trends and variability.

3.6 References

1. US Environmental Protection Agency *National Ambient Air Quality Standard for Ozone; final Rule-2015*; 2015; Vol. 80;.

2. US Environmental Protection Agency *National ambient air quality standards for ozone; final rule-2008*; 2008; Vol. 73;.

3. Simon, H.; Reff, A.; Wells, B.; Xing, J.; Frank, N. Ozone trends across the United States over a period of decreasing NOx and VOC emissions. *Environ. Sci. Technol.* **2015**, *49*, 186–195, doi:10.1021/es504514z.

4. Parrish, D. D.; Law, K. S.; Staehelin, J.; Derwent, R.; Cooper, O. R.; Tanimoto, H.; Volz-Thomas, A.; Gilge, S.; Scheel, H.-E.; Steinbacher, M.; Chan, E. Long-term changes in

lower tropospheric baseline ozone concentrations at northern mid-latitudes. *Atmos. Chem. Phys.* **2012**, *12*, 11485–11504, doi:10.5194/acp-12-11485-2012.

5. Jacob, D. J.; Logan, J. A.; Murti, P. P. Effect of rising Asian emissions on surface ozone in the United States. *Geophys. Res. Lett.* **1999**, *26*, 2175–2178, doi:10.1029/1999GL900450.

6. Lin, M.; Fiore, A. M.; Horowitz, L. W.; Langford, A. O.; Oltmans, S. J.; Tarasick, D.; Rieder, H. E. Climate variability modulates western US ozone air quality in spring via deep stratospheric intrusions. *Nat. Commun.* **2015**, *6*, 7105–7116, doi:10.1038/ncomms8105.

7. Lin, M.; Horowitz, L. W.; Payton, R.; Fiore, A. M.; Tonnesen, G. US surface ozone trends and extremes from 1980 to 2014: quantifying the roles of rising Asian emissions, domestic controls, wildfires, and climate. *Atmos. Chem. Phys.* **2017**, *17*, 2943–2970, doi:10.5194/acp-17-2943-2017.

8. Lin, M.; Horowitz, L. W.; Oltmans, S. J.; Fiore, A. M.; Fan, S. Tropospheric ozone trends at Mauna Loa Observatory tied to decadal climate variability. *Nat. Geosci.* **2014**, *7*, 136–143, doi:10.1038/ngeo2066.

9. Cooper, O. R.; Gao, R. S.; Tarasick, D.; Leblanc, T.; Sweeney, C. Long-term ozone trends at rural ozone monitoring sites across the United States, 1990-2010. *J. Geophys. Res. Atmos.* **2012**, *117*, D22307, doi:10.1029/2012JD018261.

10. Oman, L. D.; Ziemke, J. R.; Douglass, A. R.; Waugh, D. W.; Lang, C.; Rodriguez, J. M.; Nielsen, J. E. The response of tropical tropospheric ozone to ENSO. *Geophys. Res. Lett.* **2011**, *38*, L13706, doi:10.1029/2011GL047865.

11. Fiore, A. M.; Naik, V.; Leibensperger, E. M. Air Quality and Climate Connections. *J. Air Waste Manage. Assoc.* **2015**, *65*, 645–685, doi:10.1080/10962247.2015.1040526.

12. Parrish, D. D.; Petropavlovskikh, I.; Oltmans, S. J. Reversal of Long-Term Trend in Baseline Ozone Concentrations at the North American West Coast. *Geophys. Res. Lett.* **2017**, *44*, 10,675-10,681, doi:10.1002/2017GL074960.

13. Zhang, L.; Jacob, D. J.; Boersma, K. F.; Jaffe, D. A.; Olson, J. R.; Bowman, K. W.; Worden, J. R.; Thompson, A. M.; Avery, M. A.; Cohen, R. C.; Dibb, J. E.; Flocke, F. M.; Fuelberg, H. E.; Huey, L. G.; McMillan, W. W.; Singh, H. B.; Weinheimer, A. J. Transpacific transport of ozone pollution and the effect of recent Asian emission increases on air quality in North America: an integrated analysis using satellite, aircraft, ozonesonde, and surface observations. *Atmos. Chem. Phys. Discuss.* **2008**, *8*, 8143–8191, doi:10.5194/acpd-8-8143-2008.

14. Lin, M.; Fiore, A. M.; Horowitz, L. W.; Cooper, O. R.; Naik, V.; Holloway, J.; Johnson, B. J.; Middlebrook, A. M.; Oltmans, S. J.; Pollack, I. B.; Ryerson, T. B.; Warner, J. X.; Wiedinmyer, C.; Wilson, J.; Wyman, B. Transport of Asian ozone pollution into surface air over the western United States in spring. *J. Geophys. Res. Atmos.* **2012**, *117*, D00V07, doi:10.1029/2011JD016961.

15. Ziemke, J. R. La Nina and El Nino—induced variabilities of ozone in the tropical lower atmosphere during 1970–2001. *Geophys. Res. Lett.* **2003**, *30*, 1142, doi:10.1029/2002GL016387.

16. Langford, A. O.; Masterst, C. D. Modulation of Middle and upper tropospheric ozone at Northern midlatitudes by the El Nino Southern Oscillation. *J. Geophys. Res.* **1998**, *25*,

2667–2670.

17. Koumoutsaris, S.; Bey, I.; Generoso, S.; Thouret, V. Influence of El Niño-Southern Oscillation on the interannual variability of tropospheric ozone in the northern midlatitudes. *J. Geophys. Res. Atmos.* **2008**, *113*, D19301, doi:10.1029/2007JD009753.

18. Parrish, D. D.; Law, K. S.; Staehelin, J.; Derwent, R.; Cooper, O. R.; Tanimoto, H.; Volz-Thomas, A.; Gilge, S.; Scheel, H.-E.; Steinbacher, M.; Chan, E. Lower tropospheric ozone at northern midlatitudes: Changing seasonal cycle. *Geophys. Res. Lett.* **2013**, *40*, 1631–1636, doi:10.1002/grl.50303.

19. Carslaw, D. C. On the changing seasonal cycles and trends of ozone at Mace Head, Ireland. *Atmos. Chem. Phys. Discuss.* **2005**, *5*, 5987–6011, doi:10.5194/acpd-5-5987-2005.

20. Bloomer, B. J.; Vinnikov, K. Y.; Dickerson, R. R. Changes in seasonal and diurnal cycles of ozone and temperature in the eastern U.S. *Atmos. Environ.* **2010**, *44*, 2543–2551, doi:10.1016/j.atmosenv.2010.04.031.

21. Monks, P. S. A review of the observations and origins of the spring ozone maximum. *Atmos. Environ.* **2000**, *34*, 3545–3561, doi:10.1016/S1352-2310(00)00129-1.

22. Wang, Y. Springtime photochemistry at northern mid and high latitudes. *J. Geophys. Res.* **2003**, *108*, 8358–8390, doi:10.1029/2002JD002227.

23. Salisbury, G.; Monks, P. S.; Bauguitte, S.; Bandy, B. J.; Penkett, S. A. A Seasonal Comparison of the Ozone Photochemistry in Clean and Polluted Air Masses at Mace Head, Ireland. *J. Atmos. Chem.* **2002**, *41*, 163–187, doi:10.1023/A:1014202229304.

24. Cooper, O. R.; Parrish, D. D.; Stohl, A.; Trainer, M.; Nédélec, P.; Thouret, V.; Cammas, J. P.; Oltmans, S. J.; Johnson, B. J.; Tarasick, D.; Leblanc, T.; McDermid, I. S.; Jaffe, D.; Gao, R.; Stith, J.; Ryerson, T.; Aikin, K.; Campos, T.; Weinheimer, A.; Avery, M. A. Increasing springtime ozone mixing ratios in the free troposphere over western North America. *Nature* **2010**, *463*, 344–348, doi:10.1038/nature08708.

25. Jonson, J. E.; Simpson, D.; Fagerli, H.; Solberg, S. Can we explain the trends in European ozone levels? *Atmos. Chem. Phys.* **2006**, *6*, 51–66, doi:10.5194/acp-6-51-2006.

26. Cooper, O. R.; Parrish, D. D.; Ziemke, J.; Balashov, N. V.; Cupeiro, M.; Galbally, I. E.; Gilge, S.; Horowitz, L.; Jensen, N. R.; Lamarque, J.-F.; Naik, V.; Oltmans, S. J.; Schwab, J.; Shindell, D. T.; Thompson, A. M.; Thouret, V.; Wang, Y.; Zbinden, R. M. Global distribution and trends of tropospheric ozone: An observation-based review. *Elem. Sci. Anthr.* **2014**, *2*, doi:10.12952/journal.elementa.000029.

27. Wu and Huang Ensemble Empirical Mode Decomposition: A Noise Assisted Data Analysis Method. *Adv. Adapt. Data Anal.* **2009**, *1*, 385–388.

28. NPS Gaseous Pollutant and Met Data Available online: https://ard-request.air-resource.com/ (accessed on Feb 5, 2018).

29. National Park Service Air Resources Division *Gaseous Pollutant Monitoring Program Quality Assurance Project Plan (QAPP)*; 2015;

30. Wu, Z.; Huang, N. E.; Long, S. R.; Peng, C.-K. On the trend, detrending, and variability of nonlinear and nonstationary time series. *Proc. Natl. Acad. Sci.* **2007**, *104*, 14889–14894, doi:10.1073/pnas.0701020104.

31. McDonald-Buller, E. C.; Allen, D. T.; Brown, N.; Jacob, D. J.; Jaffe, D.; Kolb, C. E.; Lefohn, A. S.; Oltmans, S.; Parrish, D. D.; Yarwood, G.; Zhang, L. Establishing Policy Relevant Background (PRB) Ozone Concentrations in the United States. *Environ. Sci. Technol.* **2011**, *45*, 9484–9497, doi:10.1021/es2022818.

32. ECMWF | Advancing global NWP through international collaboration Available online: https://www.ecmwf.int/ (accessed on Feb 5, 2018).

33. Draxler, R.; Stunder, B.; Rolph, G.; Stein, A.; Taylor, A. HYSPLIT4 User's Guide. *Natl. Ocean. Atmos. Adm. Tech. Memo.* **2016**.

34. Derwent, R. G.; Jenkin, M. E.; Saunders, S. M.; Pilling, M. J. Photochemical ozone creation potentials for organic compounds in northwest Europe calculated with a master chemical mechanism. *Atmos. Environ.* **1998**, *32*, 2429–2441, doi:10.1016/S1352-2310(98)00053-3.

35. Papineau, J. M. Wintertime temperature anomalies in Alaska correlated with ENSO and PDO. *Int. J. Climatol.* **2001**, *21*, 1577–1592, doi:10.1002/joc.686.

36. Zhang, A.; Jia, G.; Epstein, H. E.; Xia, J. ENSO elicits opposing responses of semi-arid vegetation between Hemispheres. *Sci. Rep.* **2017**, *7*, 42281–42290, doi:10.1038/srep42281.

37. Stuecker, M. F.; Timmermann, A.; Jin, F.-F.; McGregor, S.; Ren, H.-L. A combination mode of the annual cycle and the El Niño/Southern Oscillation. *Nat. Geosci.* **2013**, *6*, 540–544, doi:10.1038/ngeo1826.

38. Newman, M.; Compo, G. P.; Alexander, M. A. ENSO-Forced Variability of the Pacific

Decadal Oscillation. *J. Clim.* **2003**, *16*, 3853–3857, doi:10.1175/1520-0442(2003)016<3853:EVOTPD>2.0.CO;2.

39. Timmermann, A.; Latif, M.; Grötzner, A.; Voss, R. Modes of climate variability as simulated by a coupled general circulation model. Part I: ENSO-like climate variability and its low-frequency modulation. *Clim. Dyn.* **1999**, *15*, 605–618, doi:10.1007/s003820050304.

40. US Environmental Protection Agency Air Pollutant Emissions Trends Data Available online: https://www.epa.gov/air-emissions-inventories/air-pollutant-emissions-trends-data (accessed on Mar 19, 2018).

41. Liu, Y.; Goodrick, S.; Heilman, W. Wildland fire emissions, carbon, and climate: Wildfire–climate interactions. *For. Ecol. Manage.* **2014**, *317*, 80–96, doi:10.1016/j.foreco.2013.02.020.

42. Abatzoglou, J. T.; Williams, A. P. Impact of anthropogenic climate change on wildfire across western US forests. *Proc. Natl. Acad. Sci.* **2016**, *113*, 11770–11775, doi:10.1073/pnas.1607171113.

43. Liu, J. C.; Mickley, L. J.; Sulprizio, M. P.; Dominici, F.; Yue, X.; Ebisu, K.; Anderson, G. B.; Khan, R. F. A.; Bravo, M. A.; Bell, M. L. Particulate air pollution from wildfires in the Western US under climate change. *Clim. Change* **2016**, *138*, 655–666, doi:10.1007/s10584-016-1762-6.

44. Barbero, R.; Abatzoglou, J. T.; Larkin, N. K.; Kolden, C. A.; Stocks, B. Climate change presents increased potential for very large fires in the contiguous United States. *Int. J. Wildl. Fire* **2015**, *24*, 892–899, doi:10.1071/WF15083.

45. Wilson, R. C.; Fleming, Z. L.; Monks, P. S.; Clain, G.; Henne, S.; Konovalov, I. B.; Szopa, S.; Menut, L. Have primary emission reduction measures reduced ozone across Europe? An analysis of European rural background ozone trends 1996-2005. *Atmos. Chem. Phys.* **2012**, *12*, 437–454, doi:10.5194/acp-12-437-2012.

46. Rodionov, S. N.; Bond, N. A.; Overland, J. E. The Aleutian Low, storm tracks, and winter climate variability in the Bering Sea. *Deep Sea Res. Part II Top. Stud. Oceanogr.* **2007**, *54*, 2560–2577, doi:10.1016/j.dsr2.2007.08.002.

47. Wilcox, L. J.; Highwood, E. J.; Dunstone, N. J. The influence of anthropogenic aerosol on multi-decadal variations of historical global climate. *Environ. Res. Lett.* **2013**, *8*, 24033–24042, doi:10.1088/1748-9326/8/2/024033.

48. Lin, M.; Fiore, A. M.; Cooper, O. R.; Horowitz, L. W.; Langford, A. O.; Levy, H.; Johnson, B. J.; Naik, V.; Oltmans, S. J.; Senff, C. J. Springtime high surface ozone events over the western United States: Quantifying the role of stratospheric intrusions. *J. Geophys. Res. Atmos.* **2012**, *117*, D00V22, doi:10.1029/2012JD018151.

49. L'Heureux, M. L. Atmospheric circulation influences on seasonal precipitation patterns in Alaska during the latter 20th century. *J. Geophys. Res.* **2004**, *109*, D06106, doi:10.1029/2003JD003845.

50. Stein, K.; Timmermann, A.; Schneider, N.; Jin, F. F.; Stuecker, M. F. ENSO seasonal synchronization theory. *J. Clim.* **2014**, *27*, 5285–5310, doi:10.1175/JCLI-D-13-00525.1.

51. NOAA ESRL Physical Sciences Division Pacific Decadal Oscillation Index Available online: https://www.esrl.noaa.gov/psd/gcos_wgsp/Timeseries/PDO/ (accessed on Sep 5, 2017).

52. Dentener, F., Keating, T., Akimoto, H. *Hemispheric Transport of 2010 Part A: Ozone and Particulate Matter*; United Nations Publication: Geneva, 2010; ISBN 978-92-1-117043-6.

53. Jaffe, D.; Anderson, T.; Covert, D.; Kotchenruther, R.; Trost, B.; Danielson, J.; Simpson, W.; Berntsen, T.; Karlsdottir, S.; Blake, D.; Harris, J.; Carmichael, G.; Uno, I. Transport of Asian air pollution to North America. *Geophys. Res. Lett.* **1999**, *26*, 711–714, doi:10.1029/1999GL900100.

54. Berntsen, T. K.; Karlsdóttir, S.; Jaffe, D. A. Influence of Asian emissions on the composition of air reaching the north western United States. *Geophys. Res. Lett.* **1999**, *26*, 2171–2174, doi:10.1029/1999GL900477.

55. Yienger, J. J.; Galanter, M.; Holloway, T. A.; Phadnis, M. J.; Guttikunda, S. K.; Carmichael, G. R.; Moxim, W. J.; Levy, H. The episodic nature of air pollution transport from Asia to North America. *J. Geophys. Res. Atmos.* **2000**, *105*, 26931–26945, doi:10.1029/2000JD900309.

56. Yienger, J.; Carmichael, G.; Phadnis, M.; Guttikunda, S.; Holloway, T.; Galanter, M.; Moxim, W.; Levy II, H. Transport of Air Pollution From Asia To North America. *Air Pollut. Model. Its Appl. XIV* **2001**, 307–313.

57. Holzer, M.; Hall, T. M.; Stull, R. B. Seasonality and weather-driven variability of transpacific transport. *J. Geophys. Res.* **2005**, *110*, D23103, doi:10.1029/2005JD006261.

58. Bond, N. A.; Harrison, D. E. ENSO's effect on Alaska during opposite phases of the Arctic Oscillation. *Int. J. Climatol.* **2006**, *26*, 1821–1841, doi:10.1002/joc.1339.

59. US Environmental Protection Agency *NOx Budget Trading Program 2003*; 2003;

Chapter 4: Conclusions

This study investigated the processes affecting the spatial and temporal variability in long-term surface ozone at 25 National Park Service sites. The EEMD technique decomposed ozone data into all the components driving variability. Four components of the ozone data set were explored for variability and the greatest factors affecting ozone concentration change across the continental U.S. and Alaska was determined. The ozone components analyzed include seasonal, interannual (El Niño Southern Oscillation), interdecadal (Pacific Decadal Oscillation), and long-term (multidecadal) variability.

Given that all data sets had greater than 10 years of data and that all processes on times scales < 10 years were removed, the residual was considered to be the trend on multidecadal time scales and was referred to as the *multidecadal* trend. The multidecadal trends across the U.S. National Parks suggested that ozone began decreasing earlier in areas that were closest to urban areas. These findings also showed that the effect of transport is far reaching beyond the local emission scale. As such, the multidecadal trends were increasing and are now decreasing at 20 of the 25 sites, while two have leveled off, two were decreasing from the start of monitoring, and one has ceased monitoring. Increasing trends were found to be between 0.001 ppbv yr^{-1} and 0.44 ppbv yr^{-1}. Of the 22 sites that exhibited decreasing trends, ozone decreased at rates between -0.02 ppbv yr^{-1} and -0.63 ppbv yr^{-1}.

The seasonal cycle is the shortest timescale analyzed in this study and has the largest variance (an average of 31.8%) of all components of the ozone data sets. At eight sites in the study domain, Peak ozone values of the seasonal component significantly decreased by 5 to 20 ppbv. Decreases in annual amplitude were more significant in the East (5-20 ppbv) than the West (5-7ppbv). In addition, the timing of ozone peak values shifted 10 to 60 days earlier at nine sites,

while minimum values shifted 14 to 34 days earlier at eight sites. The changes seen in the seasonal cycle were likely the result of decreasing NO_x concentrations. As mentioned previously, a decrease in NO_x decreases the frequency of high ozone events in the summer but increases ozone in the early spring and winter. This ultimately results in an increase in minimum ozone values, a decrease in maximum ozone values, and a shift in some extreme values to earlier in the year. Analysis of lower frequency components, ENSO and PDO, revealed a modulating effect on a higher frequency component, the seasonal cycle. When ENSO and PDO were acting in phase, the seasonal cycle was enhanced by increasing the annual peaks and lowering annual minimums by 3-4 ppbv compared to when the two components were acting out-of-phase.

An analysis of DENA-HQ, in Alaska revealed intriguing results. The EPA annual DM8HA, significantly increased at DENA-HQ at a rate of 0.33 ppbv yr^{-1}. This site was the only site that had a significant positive trend in the annual DM8HA value. In addition, this site had a significant increase in annual amplitude where the annual maximum had increased by 2 ppbv and the annual minimum decreased by the same amount. Therefore, the annual amplitude increased by 4 ppbv between 1987 and 2015. It was also found that the change in the PDO regime from positive to negative resulted in stronger and more frequent La Niña's between 1999 and 2015. This led to an anomalously low-pressure system over the region when transport is at its strongest, in April and May. During this period, the frequency of southwesterly wind increased by 13%. This change indicated a likely increase in transport of polluted air masses from East Asia to DENA-HQ.

From this study, we learned that on multidecadal timescales EPA ozone standards are effective, and more so near areas of higher population. This is reasonable given that prior to the implementation of ozone standards, high concentrations of precursor emissions in urban regions

traveled to NPS monitoring sites, resulting in higher concentrations of ozone. As concentrations of precursor emissions in urban areas decreased, lower concentrations of ozone occurred in NPS sites, by the same mechanism. Further study is required to understand the variabilities found in the magnitude of the annual amplitude and timing of annual peaks and minimums. The findings in these variables did not have as clear of a pattern as that found in the multidecadal trends.

Decreasing NO_x concentrations explains the change in timing of peaks from summer to spring and the decrease in annual amplitude. However, it does not explain why significant changes in these variables were not seen for all sites in a region. For example, in central California, PINN-ES and SEKI-LK had significant decreases in annual amplitude while YOSE-TD did not. This is also the case for this geographical area regarding the timing of peak and minimum annual ozone. For the same sites, PINN-ES had a significantly earlier occurring peak date while the date of peak ozone for SEKI-LK and YOSE-TD did not have significant changes. Despite the lack of regional similarities, knowing that peak ozone is occurring earlier for an area will assist policy makers in preparing the public for high ozone events at appropriate times. It can also help policy makers target and decrease high ozone concentrations. At this time, large energy plants have a budget for the amount of NOx that can be emitted from the plant during the ozone season of May to September. The period that the budget applies may need to be expanded given that ozone peaks are now occurring in April at some sites in the study domain.

Analysis of large-scale climate oscillation allowed for the quantification of the contribution of these components to the seasonal cycle. Variability in these climate modes changed atmospheric transport patterns to a site in Alaska. In a future study, the total contribution by these climate modes to all higher frequency components should be considered. The effect of changing transport patterns in response to variability in climate modes and

transported emission levels should also be quantified at all sites. In addition, a more precise determination of the point of origin of ozone promoting pollutants transported to Alaska would inform future global policy decisions.

Literature Cited

Abatzoglou, J. T., & Williams, A. P. (2016). Impact of anthropogenic climate change on wildfire across western US forests. *Proceedings of the National Academy of Sciences*, *113*(42), 11770–11775. https://doi.org/10.1073/pnas.1607171113

Barbero, R., Abatzoglou, J. T., Larkin, N. K., Kolden, C. A., & Stocks, B. (2015). Climate change presents increased potential for very large fires in the contiguous United States. *International Journal of Wildland Fire*, *24*(7), 892–899. https://doi.org/10.1071/WF15083

Baylon, P. M., Jaffe, D. A., Pierce, R. B., & Gustin, M. S. (2016). Interannual Variability in Baseline Ozone and Its Relationship to Surface Ozone in the Western U.S. *Environmental Science & Technology*, *50*(6), 2994–3001. https://doi.org/10.1021/acs.est.6b00219

Berntsen, T. K., Karlsdóttir, S., & Jaffe, D. A. (1999). Influence of Asian emissions on the composition of air reaching the north western United States. *Geophysical Research Letters*, *26*(14), 2171–2174. https://doi.org/10.1029/1999GL900477

Bloomer, B. J., Vinnikov, K. Y., & Dickerson, R. R. (2010). Changes in seasonal and diurnal cycles of ozone and temperature in the eastern U.S. *Atmospheric Environment*, *44*(21–22), 2543–2551. https://doi.org/10.1016/j.atmosenv.2010.04.031

Bond, N. A., & Harrison, D. E. (2006). ENSO's effect on Alaska during opposite phases of the Arctic Oscillation. *International Journal of Climatology*, *26*(13), 1821–1841. https://doi.org/10.1002/joc.1339

Carslaw, D. C. (2005). On the changing seasonal cycles and trends of ozone at Mace Head, Ireland. *Atmospheric Chemistry and Physics Discussions*, *5*(4), 5987–6011. https://doi.org/10.5194/acpd-5-5987-2005

Chameides, W., & Walker, J. C. G. (1973). A photochemical theory of tropospheric ozone.

Journal of Geophysical Research, *78*(36), 8751–8760. https://doi.org/10.1029/JC078i036p08751

Chandra, S., Ziemke, J. R., Min, W., & Read, W. G. (1998). Effects of 1997-1998 El Niño on tropospheric ozone and water vapor. *Geophysical Research Letters*, *25*(20), 3867–3870. https://doi.org/10.1029/98GL02695

Cooper, O. R. (2015). Trends in northern hemisphere ozone since the 1970s and the rise in baseline ozone observed across western North America Background vs Baseline ozone, 1–37.

Cooper, O. R., Gao, R. S., Tarasick, D., Leblanc, T., & Sweeney, C. (2012). Long-term ozone trends at rural ozone monitoring sites across the United States, 1990-2010. *Journal of Geophysical Research Atmospheres*, *117*, D22307. https://doi.org/10.1029/2012JD018261

Cooper, O. R., Parrish, D. D., Stohl, A., Trainer, M., Nédélec, P., Thouret, V., … Avery, M. A. (2010). Increasing springtime ozone mixing ratios in the free troposphere over western North America. *Nature*, *463*(7279), 344–348. https://doi.org/10.1038/nature08708

Cooper, O. R., Parrish, D. D., Ziemke, J., Balashov, N. V., Cupeiro, M., Galbally, I. E., … Zbinden, R. M. (2014). Global distribution and trends of tropospheric ozone: An observation-based review. *Elementa: Science of the Anthropocene*, *2*. https://doi.org/10.12952/journal.elementa.000029

Crutzen, P. J. (1974). Photochemical reactions initiated by and influencing ozone in unpolluted tropospheric air. *Tellus*, *26*(1–2), 47–57. https://doi.org/10.1111/j.2153-3490.1974.tb01951.x

D.D. Parrish et. al. (2014). Long-term changes in lower tropospheric baseline ozone concentrations: Comparing chemistry-climate models and observations at northern

midlatitudes. *Journal of Geophysical Research : Atmospheres*, *119*(2), 5719–5736. https://doi.org/10.1002/2013JD021060.Received

Dentener, F., Keating, T., Akimoto, H. (2010). *Hemispheric Transport of 2010 Part A: Ozone and Particulate Matter*. Geneva: United Nations Publication.

Derwent, R. G., Jenkin, M. E., Saunders, S. M., & Pilling, M. J. (1998). Photochemical ozone creation potentials for organic compounds in northwest Europe calculated with a master chemical mechanism. *Atmospheric Environment*, *32*(14–15), 2429–2441. https://doi.org/10.1016/S1352-2310(98)00053-3

Draxler, R., Stunder, B., Rolph, G., Stein, A., & Taylor, A. (2016). HYSPLIT4 User's Guide. *National Oceanic Atmospheric Administration Technical Memorandum*, (February). Retrieved from http://www.arl.noaa.gov/documents/reports/hysplit_user_guide.pdf

ECMWF | Advancing global NWP through international collaboration. (n.d.). Retrieved February 5, 2018, from https://www.ecmwf.int/

EPA. (2006). *Air Quality Criteria for Ozone and Related Photochemical Oxidants Volume I of III*. *Environmental Protection* (Vol. I). https://doi.org/EPA/600/R-05/004aF

Fiore, A. M., Naik, V., & Leibensperger, E. M. (2015). Air Quality and Climate Connections. *Journal of the Air & Waste Management Association*, *65*(6), 645–685. https://doi.org/10.1080/10962247.2015.1040526

Fu, C., Qian, C., & Wu, Z. (2011). Projection of global mean surface air temperature changes in next 40 years: Uncertainties of climate models and an alternative approach. *Science China Earth Sciences*, *54*(9), 1400–1406. https://doi.org/10.1007/s11430-011-4235-9

Guo, B., Chen, Z., Guo, J., Liu, F., Chen, C., & Liu, K. (2016). Analysis of the Nonlinear Trends and Non-Stationary Oscillations of Regional Precipitation in Xinjiang, Northwestern China,

Using Ensemble Empirical Mode Decomposition. *International Journal of Environmental Research and Public Health*, *13*(3), 345–365. https://doi.org/10.3390/ijerph13030345

Holzer, M., Hall, T. M., & Stull, R. B. (2005). Seasonality and weather-driven variability of transpacific transport. *Journal of Geophysical Research*, *110*, D23103. https://doi.org/10.1029/2005JD006261

IPCC. (2014). *Climate Change 2014: Mitigation of Climate Change. Summary for Policymakers and Technical Summary*. *Climate Change 2014: Mitigation of Climate Change. Part of the Working Group III Contribution to the Fifth Assessment Report of the Intergovernmental Panel on Climate Change.* https://doi.org/10.1017/CBO9781107415416.005

Jacob, D. J., Logan, J. A., & Murti, P. P. (1999). Effect of rising Asian emissions on surface ozone in the United States. *Geophysical Research Letters*, *26*(14), 2175–2178. https://doi.org/10.1029/1999GL900450

Jaffe, D., Anderson, T., Covert, D., Kotchenruther, R., Trost, B., Danielson, J., … Uno, I. (1999). Transport of Asian air pollution to North America. *Geophysical Research Letters*, *26*(6), 711–714. https://doi.org/10.1029/1999GL900100

Jaffe, D., & Ray, J. (2007). Increase in surface ozone at rural sites in the western US. *Atmospheric Environment*, *41*(26), 5452–5463. https://doi.org/10.1016/j.atmosenv.2007.02.034

Ji, F., Wu, Z., Huang, J., & Chassignet, E. P. (2014). Evolution of land surface air temperature trend. *Nature Climate Change*, *4*(6), 462–466. https://doi.org/10.1038/nclimate2223

Jonson, J. E., Simpson, D., Fagerli, H., & Solberg, S. (2006). Can we explain the trends in European ozone levels? *Atmospheric Chemistry and Physics*, *6*(1), 51–66. https://doi.org/10.5194/acp-6-51-2006

Junge, C. E. (1962). Global ozone budget and exchange between stratosphere and troposphere. *Tellus*, *14*(4), 363–377. https://doi.org/10.3402/tellusa.v14i4.9563

Kangasjarvi, J., Jaspers, P., & Kollist, H. (2005). Signalling and cell death in ozone-exposed plants. *Plant, Cell and Environment*, *28*(8), 1021–1036. https://doi.org/10.1111/j.1365-3040.2005.01325.x

Koumoutsaris, S., Bey, I., Generoso, S., & Thouret, V. (2008). Influence of El Niño-Southern Oscillation on the interannual variability of tropospheric ozone in the northern midlatitudes. *Journal of Geophysical Research Atmospheres*, *113*, D19301. https://doi.org/10.1029/2007JD009753

L'Heureux, M. L. (2004). Atmospheric circulation influences on seasonal precipitation patterns in Alaska during the latter 20th century. *Journal of Geophysical Research*, *109*, D06106. https://doi.org/10.1029/2003JD003845

Langford, A. O., & Masterst, C. D. (1998). Modulation of Middle and upper tropospheric ozone at Northern midlatitudes by the El Nino Southern Oscillation. *Journal of Geophysical Research*, *25*(14), 2667–2670.

Lefohn, A. S., Shadwick, D., & Oltmans, S. J. (2010). Characterizing changes in surface ozone levels in metropolitan and rural areas in the United States for 1980–2008 and 1994–2008. *Atmospheric Environment*, *44*(39), 5199–5210. https://doi.org/10.1016/j.atmosenv.2010.08.049

Lin, M., Fiore, A. M., Cooper, O. R., Horowitz, L. W., Langford, A. O., Levy, H., … Senff, C. J. (2012). Springtime high surface ozone events over the western United States: Quantifying the role of stratospheric intrusions. *Journal of Geophysical Research: Atmospheres*, *117*, D00V22. https://doi.org/10.1029/2012JD018151

Lin, M., Fiore, A. M., Horowitz, L. W., Cooper, O. R., Naik, V., Holloway, J., … Wyman, B. (2012). Transport of Asian ozone pollution into surface air over the western United States in spring. *Journal of Geophysical Research: Atmospheres*, *117*, D00V07. https://doi.org/10.1029/2011JD016961

Lin, M., Fiore, A. M., Horowitz, L. W., Langford, A. O., Oltmans, S. J., Tarasick, D., & Rieder, H. E. (2015). Climate variability modulates western US ozone air quality in spring via deep stratospheric intrusions. *Nature Communications*, *6*(1), 7105–7116. https://doi.org/10.1038/ncomms8105

Lin, M., Horowitz, L. W., Oltmans, S. J., Fiore, A. M., & Fan, S. (2014). Tropospheric ozone trends at Mauna Loa Observatory tied to decadal climate variability. *Nature Geoscience*, *7*(2), 136–143. https://doi.org/10.1038/ngeo2066

Lin, M., Horowitz, L. W., Payton, R., Fiore, A. M., & Tonnesen, G. (2017). US surface ozone trends and extremes from 1980 to 2014: quantifying the roles of rising Asian emissions, domestic controls, wildfires, and climate. *Atmospheric Chemistry and Physics*, *17*, 2943–2970. https://doi.org/10.5194/acp-17-2943-2017

Liu, J. C., Mickley, L. J., Sulprizio, M. P., Dominici, F., Yue, X., Ebisu, K., … Bell, M. L. (2016). Particulate air pollution from wildfires in the Western US under climate change. *Climatic Change*, *138*(3–4), 655–666. https://doi.org/10.1007/s10584-016-1762-6

Liu, Y., Goodrick, S., & Heilman, W. (2014). Wildland fire emissions, carbon, and climate: Wildfire–climate interactions. *Forest Ecology and Management*, *317*, 80–96. https://doi.org/10.1016/j.foreco.2013.02.020

McDonald-Buller, E. C., Allen, D. T., Brown, N., Jacob, D. J., Jaffe, D., Kolb, C. E., … Zhang, L. (2011). Establishing Policy Relevant Background (PRB) Ozone Concentrations in the

United States. *Environmental Science & Technology*, *45*(22), 9484–9497. https://doi.org/10.1021/es2022818

Monks, P. S. (2000). A review of the observations and origins of the spring ozone maximum. *Atmospheric Environment*, *34*(21), 3545–3561. https://doi.org/10.1016/S1352-2310(00)00129-1

Monks, P. S., Granier, C., Fuzzi, S., Stohl, A., Williams, M. L., Akimoto, H., … von Glasow, R. (2009). Atmospheric composition change – global and regional air quality. *Atmospheric Environment*, *43*(33), 5268–5350. https://doi.org/10.1016/j.atmosenv.2009.08.021

National Park Service. (2016). Ozone and Meteorology Monitoring. Retrieved March 10, 2018, from https://www.nature.nps.gov/air/monitoring/network.cfm

National Park Service Air Resources Division. (2015). *Gaseous Pollutant Monitoring Program Quality Assurance Project Plan (QAPP).*

Newman, M., Compo, G. P., & Alexander, M. A. (2003). ENSO-Forced Variability of the Pacific Decadal Oscillation. *Journal of Climate*, *16*(23), 3853–3857. https://doi.org/10.1175/1520-0442(2003)016<3853:EVOTPD>2.0.CO;2

NOAA. (2017). NOAA: La Niña ends, increasing odds El Niño will return winter 2017-2018. Retrieved March 20, 2018, from https://addins.wpta21.com/blogs/weather/noaa-la-nina-ends-increasing-odds-el-nino-will-return-winter-2017-2018/

NOAA ESRL Physical Sciences Division. (n.d.). Pacific Decadal Oscillation Index. Retrieved September 5, 2017, from https://www.esrl.noaa.gov/psd/gcos_wgsp/Timeseries/PDO/

NPS Gaseous Pollutant and Met Data. (n.d.). Retrieved February 5, 2018, from https://ard-request.air-resource.com/

Oltmans, S. J., Lefohn, A. S., Harris, J. M., Galbally, I., Scheel, H. E., Bodeker, G., … Cuevas,

E. (2006). Long-term changes in tropospheric ozone. *Atmospheric Environment*, *40*(17), 3156–3173. https://doi.org/10.1016/j.atmosenv.2006.01.029

Oman, L. D., Ziemke, J. R., Douglass, A. R., Waugh, D. W., Lang, C., Rodriguez, J. M., & Nielsen, J. E. (2011). The response of tropical tropospheric ozone to ENSO. *Geophysical Research Letters*, *38*, L13706. https://doi.org/10.1029/2011GL047865

Papineau, J. M. (2001). Wintertime temperature anomalies in Alaska correlated with ENSO and PDO. *International Journal of Climatology*, *21*, 1577–1592. https://doi.org/10.1002/joc.686

Parrish, D. D., Law, K. S., Staehelin, J., Derwent, R., Cooper, O. R., Tanimoto, H., … Chan, E. (2012). Long-term changes in lower tropospheric baseline ozone concentrations at northern mid-latitudes. *Atmospheric Chemistry and Physics*, *12*(23), 11485–11504. https://doi.org/10.5194/acp-12-11485-2012

Parrish, D. D., Law, K. S., Staehelin, J., Derwent, R., Cooper, O. R., Tanimoto, H., … Chan, E. (2013). Lower tropospheric ozone at northern midlatitudes: Changing seasonal cycle. *Geophysical Research Letters*, *40*(8), 1631–1636. https://doi.org/10.1002/grl.50303

Parrish, D. D., Petropavlovskikh, I., & Oltmans, S. J. (2017). Reversal of Long-Term Trend in Baseline Ozone Concentrations at the North American West Coast. *Geophysical Research Letters*, *44*(20), 10,675-10,681. https://doi.org/10.1002/2017GL074960

Rodionov, S. N., Bond, N. A., & Overland, J. E. (2007). The Aleutian Low, storm tracks, and winter climate variability in the Bering Sea. *Deep Sea Research Part II: Topical Studies in Oceanography*, *54*(23–26), 2560–2577. https://doi.org/10.1016/j.dsr2.2007.08.002

Ross, J. (2009). The Pacific Ocean's Influence on Climate Change: How Low Will the PDO Go? Retrieved March 20, 2018, from https://www.sott.net/article/183250-The-Pacific-Oceans-Influence-on-Climate-Change-How-Low-Will-the-PDO-Go

Salisbury, G., Monks, P. S., Bauguitte, S., Bandy, B. J., & Penkett, S. A. (2002). A Seasonal Comparison of the Ozone Photochemistry in Clean and Polluted Air Masses at Mace Head, Ireland. *Journal of Atmospheric Chemistry*, *41*(2), 163–187. https://doi.org/10.1023/A:1014202229304

Seinfeld, JH; Pandis, S. (2006). *Atmospheric Chemistry and Physics: from Air Pollution to Climate Change* (second, Vol. 52). Wiley. Retrieved from http://www.sciencelib.net/files/Atmospheric Chemistry and Physics 2nd ed - J. Seinfeld%2C S. Pandis %28Wiley%2C 2006%29 WW.pdf

Seinfeld, J. H., & Pandis, S. N. (2006). *ATMOSPHERIC From Air Pollution to Climate Change SECOND EDITION*.

Sillman, S. (1999). The relation between ozone, NO(x) and hydrocarbons in urban and polluted rural environments. *Atmospheric Environment*, *33*(12), 1821–1845. https://doi.org/10.1016/S1352-2310(98)00345-8

Sillman, S. (2003). *Overview: tropospheric ozone, smog and ozone-NOx-VOC sensitivity*. *University of Michigan*.

Simon, H., Reff, A., Wells, B., Xing, J., & Frank, N. (2015). Ozone trends across the United States over a period of decreasing NOx and VOC emissions. *Environmental Science and Technology*, *49*(1), 186–195. https://doi.org/10.1021/es504514z

Stein, K., Timmermann, A., Schneider, N., Jin, F. F., & Stuecker, M. F. (2014). ENSO seasonal synchronization theory. *Journal of Climate*, *27*(14), 5285–5310. https://doi.org/10.1175/JCLI-D-13-00525.1

Stevenson, D. S., Dentener, F. J., Schultz, M. G., Ellingsen, K., van Noije, T. P. C., Wild, O., … Szopa, S. (2006). Multimodel ensemble simulations of present-day and near-future

tropospheric ozone. *Journal of Geophysical Research*, *111*(D8), D08301. https://doi.org/10.1029/2005JD006338

Stohl, A. (2003). Stratosphere-troposphere exchange: A review, and what we have learned from STACCATO. *Journal of Geophysical Research*, *108*(D12), 8516. https://doi.org/10.1029/2002JD002490

Stuecker, M. F., Timmermann, A., Jin, F.-F., McGregor, S., & Ren, H.-L. (2013). A combination mode of the annual cycle and the El Niño/Southern Oscillation. *Nature Geoscience*, *6*(7), 540–544. https://doi.org/10.1038/ngeo1826

Timmermann, A., Latif, M., Grötzner, A., & Voss, R. (1999). Modes of climate variability as simulated by a coupled general circulation model. Part I: ENSO-like climate variability and its low-frequency modulation. *Climate Dynamics*, *15*(8), 605–618. https://doi.org/10.1007/s003820050304

U.S. Department of the Interior National Park Service. (2010). *Air Quality in National Parks, 2008 Annual Performance & Progress Report*.

U.S. EPA. (2015). Air Quality Guide for Ozone. Retrieved April 24, 2018, from https://www.airnow.gov/index.cfm?action=pubs.aqiguideozone

US Department of Commerce, N. E. S. R. L. C. S. D. (n.d.). Scientific Assessment of Ozone Depletion 1994 - Common Questions About Ozone. Retrieved from https://www.esrl.noaa.gov/csd/assessments/ozone/1994/common_questions.html

US Environmental Protection Agency. (2003). *NOx Budget Trading Program 2003*. *Baseline*.

US Environmental Protection Agency. (2008). *National ambient air quality standards for ozone; final rule-2008*. *Federal Register* (Vol. 73).

US Environmental Protection Agency. (2014). *Policy Assessment for the Review of the Ozone*

National Ambient Air Quality Standards. *US Environmental Protection Agency*. Retrieved from http://www.epa.gov/ttn/naaqs/standards/ozone/data/20140829pa.pdf

US Environmental Protection Agency. (2015a). *National Ambient Air Quality Standard for Ozone; final Rule-2015* (Vol. 80).

US Environmental Protection Agency. (2015b). *Overview of EPA's Updates to the Air Quality Standards for Ground-Level Ozone*.

US Environmental Protection Agency. (2017). Air Pollutant Emissions Trends Data. Retrieved March 19, 2018, from https://www.epa.gov/air-emissions-inventories/air-pollutant-emissions-trends-data

US Environmental Protection Agency. (2018). Class 1 Areas - Data.gov. Retrieved February 1, 2018, from https://catalog.data.gov/dataset/class-1-areas

US EPA. (2015). *Epa's 2015 ozone standard: concerns over science and implementation*. Washington, DC.

Vingarzan, R. (2004). A review of surface ozone background levels and trends. *Atmospheric Environment*, *38*(21), 3431–3442. https://doi.org/10.1016/j.atmosenv.2004.03.030

Wang, H., Kumar, A., Wang, W., & Xue, Y. (2012). Seasonality of the Pacific Decadal Oscillation. *Journal of Climate*, *25*(1), 25–38. https://doi.org/10.1175/2011JCLI4092.1

Wang, Y. (2003). Springtime photochemistry at northern mid and high latitudes. *Journal of Geophysical Research*, *108*(D4), 8358–8390. https://doi.org/10.1029/2002JD002227

Wilcox, L. J., Highwood, E. J., & Dunstone, N. J. (2013). The influence of anthropogenic aerosol on multi-decadal variations of historical global climate. *Environmental Research Letters*, *8*(2), 24033–24042. https://doi.org/10.1088/1748-9326/8/2/024033

Wilson, R. C., Fleming, Z. L., Monks, P. S., Clain, G., Henne, S., Konovalov, I. B., … Menut, L.

(2012). Have primary emission reduction measures reduced ozone across Europe? An analysis of European rural background ozone trends 1996-2005. *Atmospheric Chemistry and Physics*, *12*(1), 437–454. https://doi.org/10.5194/acp-12-437-2012

Wu, Z., Huang, N. E., Long, S. R., & Peng, C.-K. (2007). On the trend, detrending, and variability of nonlinear and nonstationary time series. *Proceedings of the National Academy of Sciences*, *104*(38), 14889–14894. https://doi.org/10.1073/pnas.0701020104

Wu, Z., Huang, N. E., Wallace, J. M., Smoliak, B. V., & Chen, X. (2011). On the time-varying trend in global-mean surface temperature. *Climate Dynamics*, *37*(3–4), 759–773. https://doi.org/10.1007/s00382-011-1128-8

Wu, Z., Schneider, E. K., Kirtman, B. P., Sarachik, E. S., Huang, N. E., & Tucker, C. J. (2008). The modulated annual cycle: an alternative reference frame for climate anomalies. *Climate Dynamics*, *31*(7–8), 823–841. https://doi.org/10.1007/s00382-008-0437-z

Wu and Huang. (2009). Ensemble Empirical Mode Decomposition: A Noise Assisted Data Analysis Method. *Advances in Adaptive Data Analysis*, *1*(1), 385–388.

Yienger, J., Carmichael, G., Phadnis, M., Guttikunda, S., Holloway, T., Galanter, M., … Levy II, H. (2001). Transport of Air Pollution From Asia To North America. *Air Pollution Modeling and Its Application XIV*, 307–313.

Yienger, J. J., Galanter, M., Holloway, T. A., Phadnis, M. J., Guttikunda, S. K., Carmichael, G. R., … Levy, H. (2000). The episodic nature of air pollution transport from Asia to North America. *Journal of Geophysical Research: Atmospheres*, *105*(D22), 26931–26945. https://doi.org/10.1029/2000JD900309

Zhang, A., Jia, G., Epstein, H. E., & Xia, J. (2017). ENSO elicits opposing responses of semi-arid vegetation between Hemispheres. *Scientific Reports*, *7*, 42281–42290.

https://doi.org/10.1038/srep42281

Zhang, L., Jacob, D. J., Boersma, K. F., Jaffe, D. A., Olson, J. R., Bowman, K. W., … Weinheimer, A. J. (2008). Transpacific transport of ozone pollution and the effect of recent Asian emission increases on air quality in North America: an integrated analysis using satellite, aircraft, ozonesonde, and surface observations. *Atmospheric Chemistry and Physics Discussions*, *8*(2), 8143–8191. https://doi.org/10.5194/acpd-8-8143-2008

Ziemke, J. R. (2003). La Nina and El Nino—induced variabilities of ozone in the tropical lower atmosphere during 1970–2001. *Geophysical Research Letters*, *30*(3), 1142. https://doi.org/10.1029/2002GL016387

Deborah F. McGlynn

mcglyndf@vt.edu
(315)-534-9696

Education:

- **Virginia Polytechnic Institute and State University**, Blacksburg, VA
  Ph.D. Civil and Environmental Engineering: Anticipated May 2021
  GPA: 3.67
- **SUNY College Environmental Science and Forestry,** Syracuse, NY
  M.S. Chemistry: Anticipated May 2018
  GPA: 3.45
- **University at Albany - SUNY**
  B.S. Environmental Science, minor in Chemistry: December 2014
  GPA: 3.47

Research experience:

- **Graduate research, SUNY ESF:** Syracuse, NY, August 2015 to current
  Advised by Dr. Huiting Mao
  - Statistical analyses
  - Use of computational models to discern emission trends
  - Technical writing
  - Maintenance and calibration of meteorological instruments
  - Mentoring of undergraduate students
- **Undergraduate thesis, SUNY Albany:** Albany, NY, Spring and fall of 2014
  Advised by Mathias Vuille Spring 2014, and Brian Rose Fall 2014
  The impact of the El Nino Southern Oscillation and the Atlantic Multidecadal Oscillation on selected glaciers in the Andes of South America
  - Statistical analysis
  - Use of Matlab to create composite maps and graphs

Work Experience:

- **Graduate Research Assistant:** Blacksburg, VA, July 2017 to present
  - Analysis of air samples using GC/MS, GC/TD, and spot sampler
  - Programming of microcontrollers for analysis of fire plume composition on UAV platform
- **General Chemistry Teaching Assistant:** Syracuse, NY, August 2015 to current
  Instruct general chemistry students in general chemistry lab
  - Analysis scientific data and student papers
  - Present lab processes to undergraduate students
- **Funding guide manager at Syracuse University Center for Excellence:** Syracuse, NY, May 2016 to June 2017
  - Determine relevant funding opportunities for partners and summarize
- **Field and Lab Technician at Atmospheric Science Research Center:** Albany NY, Summer 2014
  - Researched gas fluxes on fresh water lakes and how it shifts with changes in biogeochemical processes
  - Maintenance and calibration of a variety of atmospheric and water quality probes
  - Use of dataloggers to record instrumental data.

Research Presentations and Publications:

- **McGlynn, D.F.,** Mao, H., Wu, Z., Sive, B., Sharac, T., "Understanding long-term-variation in surface ozone in United States (U.S.) National Parks," *Atmosphere*, vol.9, no. 4, **2018**, p.125, doi:10.3390/atmos9040125
- **McGlynn, D**., Vuille, M., Rose, B., "The impact of the El Nino Southern Oscillation and the Atlantic Multidecadal Oscillation on selected glaciers in the Andes of South America", December 12th, 2014, University at Albany Honor's Thesis Seminar

Honors and Awards:

- Undergraduate Merit Scholarship for leadership, $12,000, Awarded May 2011 from anonymous
- National Society of Collegiate Scholars, 2012-2014
- Presidential Honor Society, 2012-2014
- SUNY Albany Dean's list, Fall 2011-December 2014

Computational Fluency:

- Algorithm development
- Geographical plots
- Statistical analyses
- R, Matlab, C^{++}, HYSPLIT, ArcGIS, Origin, Python, Excel